MARMARA UNIVERSITY
FACULTY OF ENGINEERING

DESIGNING THRUST VECTOR CONTROL FOR A 6DOF MODEL ROCKET

Mert ÖZAY

GRADUATION PROJECT REPORT

Department of Mechanical Engineering

Supervisors
Assist. Prof. Dr. Uğur TÜMERDEM & Assist. Prof. Dr. Sina Kuseyri

ISTANBUL, 2023

MARMARA UNIVERSITY
FACULTY OF ENGINEERING

Designing Thrust Vector Control for a 6DOF Model Rocket

by

Mert ÖZAY

January 26, 2023, Istanbul

SUBMITTED TO THE DEPARTMENT OF MECHANICAL ENGINEERING IN PARTIAL FULFILLMENT OF THE REQUIREMENTS FOR THE DEGREE

OF

BACHELOR OF SCIENCE

AT

MARMARA UNIVERSITY

Signature of Author(s) ....M. ÖZAY..........
Department of Mechanical Engineering

Certified By ....
Project Supervisor, Department of Mechanical Engineering

Accepted By..
Head of the Department of Mechanical Engineering

ACKNOWLEDGEMENT

First of all, I would like to thank my supervisors Assist. Prof. Dr. Uğur Tümerdem and Assist. Prof. Dr. Sina Kuseyri for the valuable guidance and advice on preparing this thesis and giving me moral and material support.

January, 2023 Mert Özay

CONTENTS

ABSTRACT

Designing Thrust Vector Control for a Model Rocket

The ability of an aircraft, missile, or other object to regulate the attitude or angular velocity of the body by manipulating the direction of thrust from its engine(s) or motor(s) is called thrust vectoring also known as thrust vector control (TVC). In aerospace applications that fly outside the Kármán line, traditional aerodynamic control surfaces such as fins are ineffective. Therefore, the main method of attitude control is thrust vectoring. To apply this method to a model rocket, a gimbal that uses two servo motor in order to rotate the solid motor by yaw and pitch axis will be used. The simulation process will take place in Simulink in order to get solid result before building the real model.

SYMBOLS

C_G: Centre of gravity

C_P: Centre of pressure

α: Angle of attack (incidence)

β: Angle of sideslip

ϕ: Roll angle

θ: Pitch angle

ψ: Yaw angle

ρ: Mass density of the air

K: Gain coefficient for quaternion

ϵ: Error term for quaternion

λ: TVC gimbal's y-axis rotation angle

μ: TVC gimbal's z-axis rotation angle

ABBREVIATIONS

TVC: Thrust Vector Control

LITVC: Liquid Injection Thrust Vector Control

DOF: Degree of Freedom

PID: Proportional Integral Derivative

CAD: Computer Aided Design

LIST OF FIGURES **PAGE**

LIST OF TABLES **PAGE**

1. INTRODUCTION

Thrust vector control has assisted in the return of people from space, the landing of multiple rovers on planets [1, 2], and the landing of an asteroid [3] and more due of the immensely advantageous ability to adjust the thrust vector of any propulsion system. Thank to these missions and many more, now we know that Mars had water at some point in its life, Titan (Saturn's moon) has lakes of methane which is an organic compound. Therefore, thrust vector control has been regarded a critical field of research in launch systems.

Fins are one of the most necessary part of the model rockets. The reason for that is fins makes the model rockets more stable since they operate deep in the atmosphere where the air is thick. However, the rockets that fly into space do not fly straight, they fly with an angle in order to increase its vertical velocity, and taking it out of the atmosphere more quickly. This reduces both aerodynamic drag as well as aerodynamic stress during launch. Also, the rockets that fly into space does not spend much time in atmosphere. Moreover, fins in vacuum are useless due to lack of air drag. In order to control the rocket, TVC is used widely with many different varieties. Such as propellant injection that uses a fluid sprayed from injectors mounted around the end of the rocket into the exhaust flow, vernier thrusters, exhaust vanes or gimbaling the nozzle via servo actuation system [4].

1.1. Aim of the Research

The ability of a rocket to manipulate the direction of the thrust from its engine(s) or motor(s) to control the attitude or angular velocity of the vehicle is a necessary attribute nowadays. The ability to follow a trajectory rather than ascending upward or in fixed angle is highly required for any spacecraft for efficiency and convenient. This being said, designing a thrust vector control for a model rocket that flies highly low compare to a real rocket like Falcon 9 is unnecessary. However, as the main idea of engineering, it is a challenge that is waiting to solve and a step for the real life application. With this research, the 6DOF flight model will be controlled using 2DOF gimbal designed by me and the main concept of 6DOF motion and thrust vectoring will be understood.

1.2. Thrust Vector Control Types

1.2.1. Propellant Injection

Liquid injection thrust vector control (LITVC) is accomplished by injecting a fluid (gas or liquid) into the main exhaust flow from injectors around the end of the rocket. This technique secures the nozzle and motor in place.

Liquid injection thrust vector control necessitates very minor changes to the rocket motor's design. The important components (servo valves, pipes, tanks, etc) are housed in shielded areas, generally around the nozzle exterior, and only require bracketry for attachment and light insulation to keep them safe from plume heat radiation. Mounting surfaces and holes through the nozzle exit cone are required for the injection valves. These are easy to design and have not cause any issues.

The key problems are accurate determination of the maximum duty cycle, finding the optimum location and geometry of injector valves for best efficiency, selecting an injectant that is high in density and available chemical energy and had matched for compatibility with materials for the nozzle walls, seals and other exposed components [5].

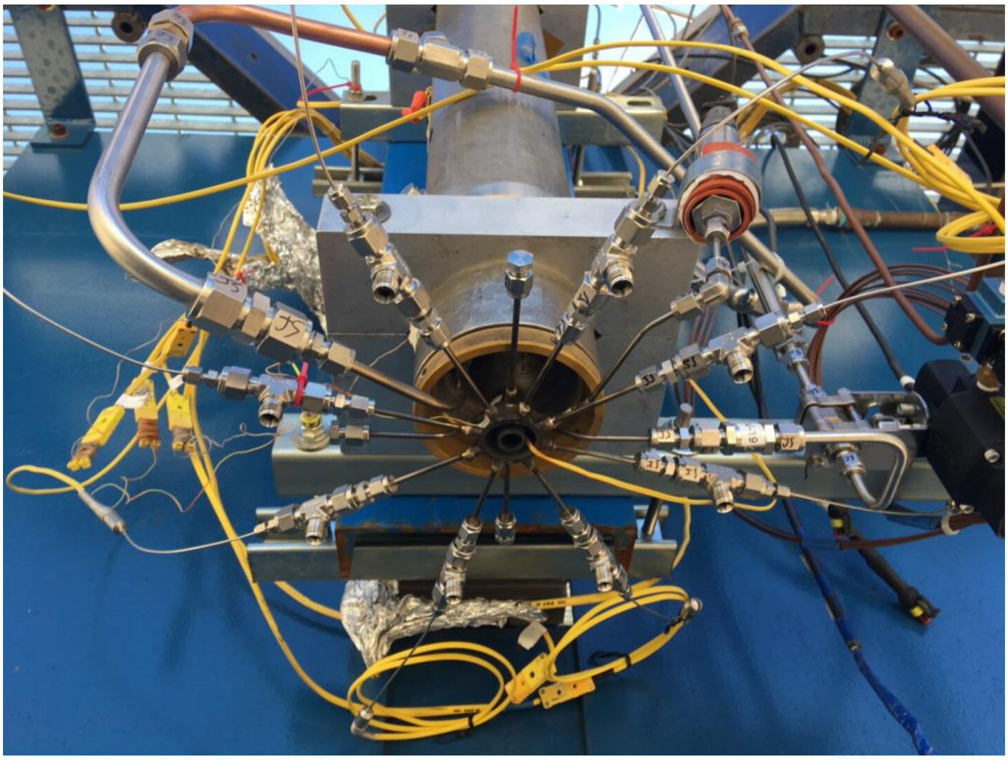

Figure 1.2.1.1 LITVC system used by Parabilis Space Technologies, Inc

1.2.2. Vernier Thrusters

A vernier thruster is a rocket engine that is used for to make fine adjustments to the velocity and attitude of a spacecraft. The size of the vernier thrusters is highly dependent on the designs of a spacecraft's manoeuvring and stability systems. It may be smaller than the main rocket engine and may complement the primary propulsion system, for example Atlas I launch vehicle [6]. Also, it may complement larger attitude control thrusters or be a part of the reaction control system. However, vernier thrusters are rarely utilized in modern designs due to their weight and the additional piping required for their functioning.

Figure 1.2.2.1 Atlas I Launch vehicle with vernier thrusters

1.2.3. Exhaust Vanes

Exhaust vanes (jet vanes) are one of the earliest TVC methods. It uses the side force created by the deflection of the vane into the exhaust jet. These exhaust vanes or jet vanes divert thrust without moving any engine components, yet they diminish the rocket's efficiency. Exhaust vanes are small, heat-resistant rudders that are attached to the nozzle exit cones aft.

An exhaust vane TVC system typically consists of four wedge-shaped configurations positioned near the nozzle's exit plane. Pitch (vertical) and yaw (side) motions are provided by the vanes opposite each other, or all four vanes can be operated simultaneously to produce torque for roll control.

In German V-2 missiles, vanes made of graphite were used [7]. Nowadays, vanes that are made of extremely heat-resistant alloys are utilized in operational propulsion systems.

Figure 1.2.3.1 V2 rocket’s exhaust vanes

1.2.4. Gimbaled Thrust

Many liquid rockets use the ability of gimbaling the whole engine in order to control the thrust. This ability contains moving the whole combustion chamber and outer engine bell, or possibly the complete engine assembly, including the fuel and oxidizer pumps.

An example to this method of TVC is Saturn V [8].

For solid propellant ballistic missiles, different method has been developed. This method achieves thrust vectoring by utilizing electric actuators or hydraulic cylinders to deflect just the rocket's nozzle. A ball joint with a hole in the middle or a flexible seal made of a thermally resistant substance connects the nozzle to the missile, with the latter requiring more torque and a higher power actuation mechanism.

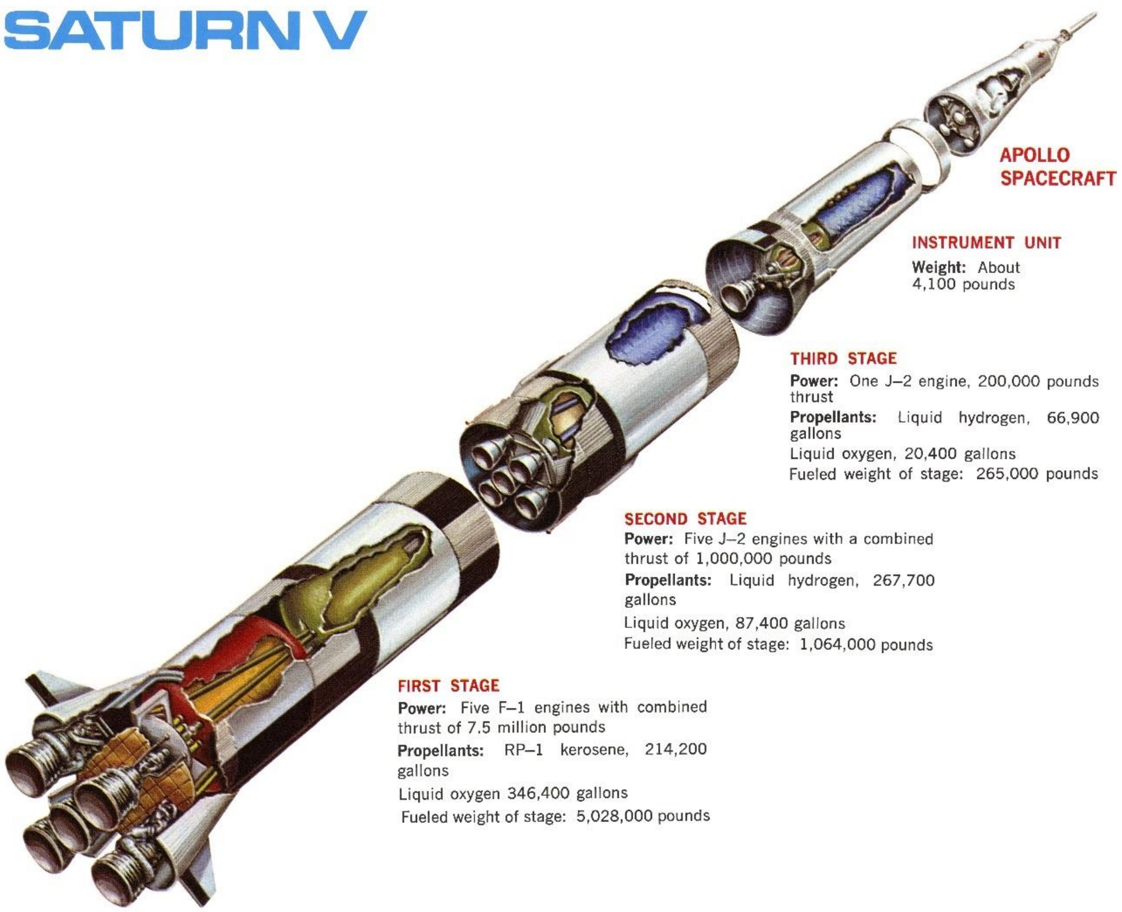

Figure 1.2.4.1 The outer engines of first and second stage and the engine on the third stage equipped with hydraulic actuated TVC gimbals on Saturn V rocket

2. ROCKET STABILITY

A minor shift in the rocket's orientation due to a gust of wind or other disturbance is possible. When this occurs, the rocket centreline is no longer parallel to the velocity of the rocket. This condition is called flying at an angle of attack α, where α is the angle between the rocket centerline and the velocity vector. A model rocket, like any other object in flight, rotates around its centre of gravity (c_g). When the rocket's body and flight path are at an angle, the body and fins of the rocket provide lift force.

As you can see on the Figure 2.1, there are three cases for which the flight direction is exactly vertical. In the centre of the figure, the rocket is undisturbed and the axis is aligned with the flight direction. The drag of the rocket is along the axis and there is no lift generated. On the left of the figure, a powered rocket has had the nose of the rocket perturbed to the right. On the right of the figure, a coasting rocket has had the nose of the rocket perturbed to the left. We denote the angle in both cases by the symbol α. Considering the powered rocket case, we see that a lift force is generated and directed towards the right or downwind side of the rocket. On the coasting rocket case, the lift is directed towards the left, also the downwind side of the rocket. For the powered case, both the lift and the drag produce counter-clockwise torques, or twists, about the centre of gravity; the tail of the rocket will swing to the right under the action of both forces and the nose will move to left. For the coasting case, both lift and drag produce clockwise torques about the centre of gravity; the tail of the rocket will swing to the left under the action of both forces and the nose will move to the right. In both cases, the lift and the drag forces move the nose back towards the flight direction. Engineers call this a restoring force because the forces "restore" the vehicle to its initial condition and the rocket is determined to be stable.

A restoring force exists for this model rocket because the centre of pressure is below the centre of gravity. If the centre of pressure is above the centre of gravity, the lift and drag forces maintain their directions but the direction of the torque generated by the forces is reversed. This is called a de-stabilizing force. Any small displacement of the nose generates forces that cause the displacement to increase. The conditions for a stable rocket are that the centre of pressure must be located below the centre of gravity.

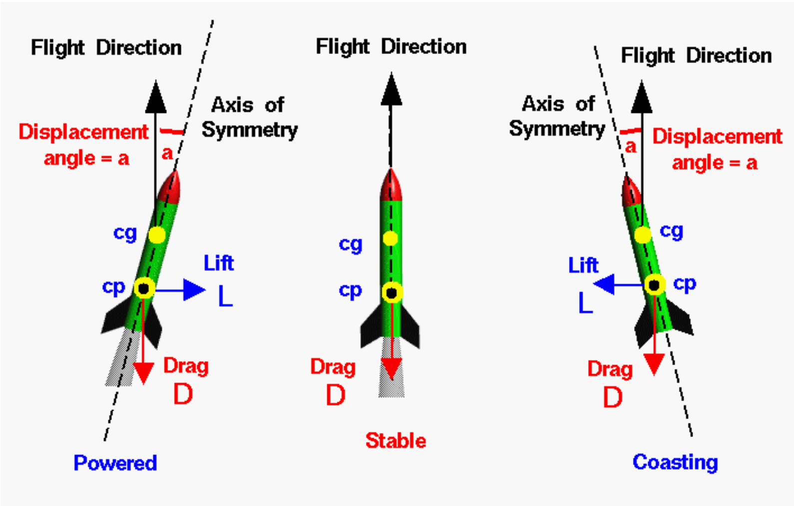

Figure 2.1 Stability of a model rocket with fins

Aerodynamics are rarely used for stability in modern full-scale rockets. The exhaust nozzles of full-scale rockets rotate to offer stability and control. That's why a Delta, Titan, or Atlas rocket doesn't have fins. When fins are absence in a model rocket, the lift force produced by the fins will be zero.

In order to understand how stable the rocket is, a dimensionless number called stability margin is used. This stability margin of a rocket can be calculated dividing the distance between the C_G and the C_P by the body tube diameter. To calculate the location of the C_P, Barrowman equation can be used [9]. For finless rockets, this stability margin value is always less negative since the C_P located higher than the C_G, relatively. This will lead to unstable flight for the model rocket.

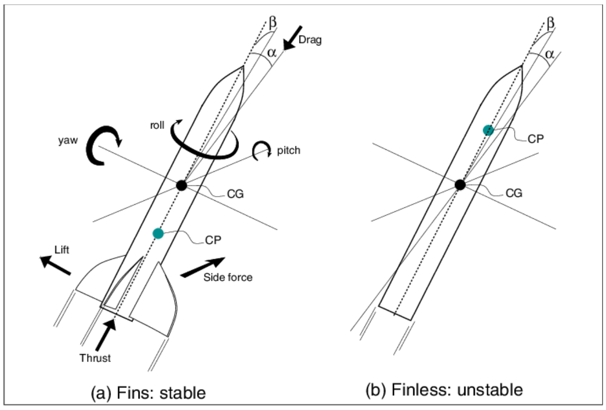

Figure 2.2 Stable and unstable rocket [10]

3. ROCKET DYNAMICS

When we are looking the forces on a body of rocket, there will be several forces to understand. These are simply weight, thrust and drag forces. To understand the rocket behaviour, second law of motion will be used.

$$\sum F = Ma \tag{1}$$

Forces at through the C_G

$$F_{gravity} = Mg \tag{2}$$

The thrust force seen by the rocket is equal to the rate of change of momentum carried away in the exhaust

$$F_{thrust} = \frac{d}{dt}(MV) \tag{3}$$

Drag is a resistance from the air to the rocket motion. There are three forms of drag, and their relative importance is highly dependent on the speed on the rocket relative to the sound speed. First one is skin friction and the contact between the fluid and the body's skin causes skin friction. Second one is pressure drag (form drag) and develops as a result of the object's shape. The most essential component in form drag is the body's overall size and shape. The drag of a body with a larger apparent cross section is greater than the drag of a body with a smaller apparent cross section. The last one is wave drag and it is generated by the production of shock waves surrounding the aircraft that radiate a significant amount of energy, increasing drag. Drag always has an effect at through the C_P [11].

3.1. Assumptions

- Flat earth model used as the earth coordinate axis.
- The atmosphere is at rest relative to the earth, and atmospheric properties are functions of altitude only.

- The thrust and other forces except weight is not taken into account while finding out the dynamic equations.
- Mass is constant throughout the flight.
- Body lift, form and wave drag is negligible since there is no fins and the scale of the flight relatively small.

The idea and the reasoning behind the last assumption derived from my first model that have all the forces all together. This caused so many complexities and made the Simulink model fairly messy.

3.2. Dynamic Equations

In order to simulate the behaviour of a thrust vector gimbal on a model rocket, the rocket and its flight behaviour analysed. To obtain the model, a body fixed coordinate system placed on the C_G of the rocket. The axis placement and names can be seen in Fig. 3.2.1 and Fig. 3.2.2. Then, acceleration terms found using second law of motion on the respective axis.

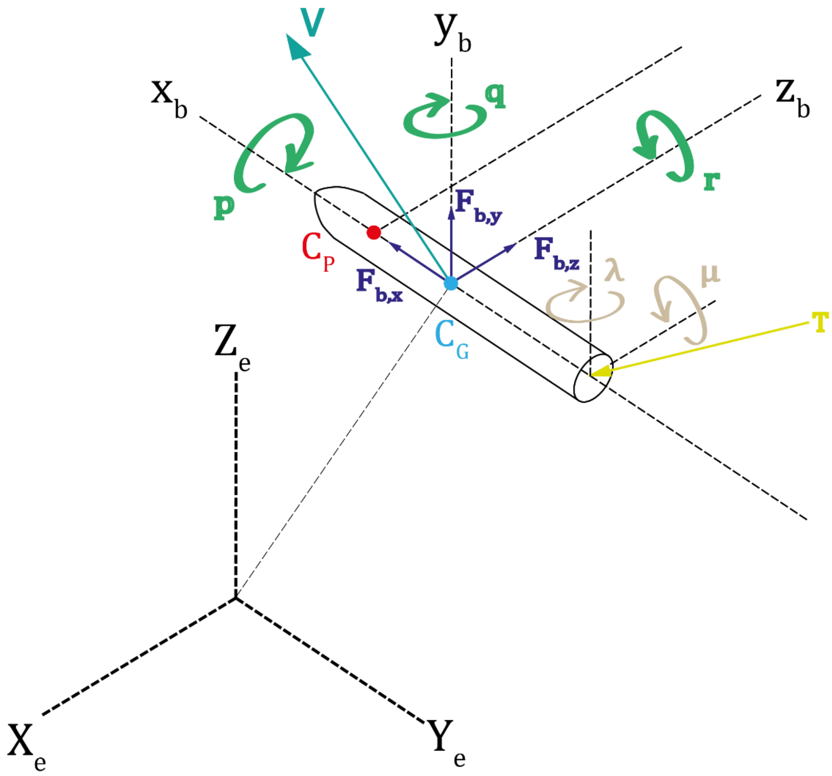

Figure 2.2.1 The inertial (earth) frame and body frame placed at the rocket's $\mathbf{C_G}$

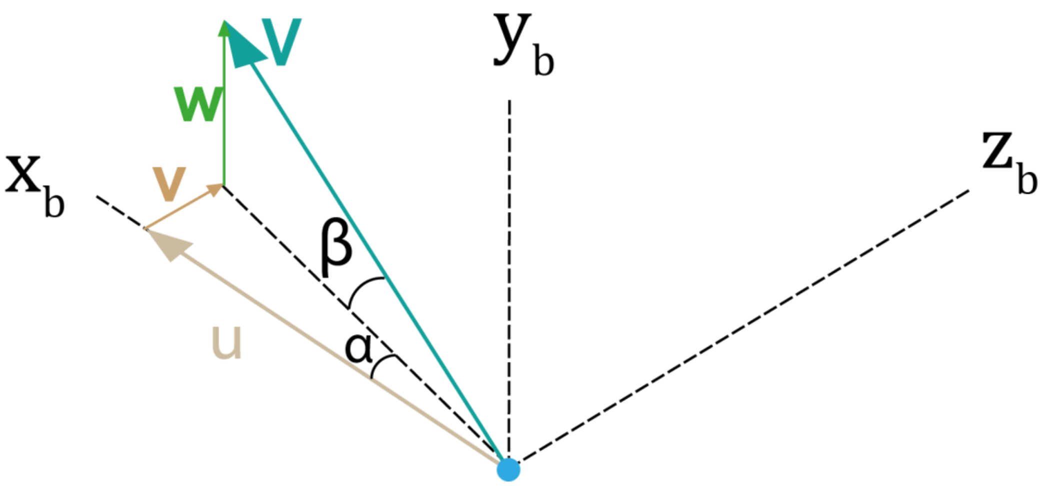

Figure 3.2.2 The velocity component in the body frame of the rocket

3.2.1. Translational Accelerations

$$F_b - W = \frac{d}{dt}(m\vec{V}) + \vec{\omega} \times (m\vec{V}) \tag{4}$$

where F_b is body forces on the body frame ($[F_x \quad F_y \quad F_z]^T$), m is mass of the rocket, W is the weight of the rocket, $\vec{V}$ is the velocity of the rocket on the body frame ($[u \quad v \quad w]^T$), $\vec{\omega}$ is the angular velocity of the rocket on the body frame ($[p \quad q \quad r]^T$)

$$m\frac{d}{dt}(\vec{V}) = F_b - W - \vec{\omega} \times (m\vec{V}) \tag{5}$$

Since the gravitational acceleration acts on the inertial (earth) frame, it needs to be transformed into the body frame in order to use it in the body frame calculations. Therefore;

$$\underbrace{\begin{bmatrix} i \\ j \\ k \end{bmatrix}}_{body\ frame} = \begin{bmatrix} c\theta c\psi & c\theta s\psi & -s\theta \\ s\phi s\theta c\psi - c\phi s\psi & s\phi s\theta s\psi + c\phi c\psi & s\phi c\theta \\ c\phi s\theta c\psi + s\phi s\psi & c\phi s\theta s\psi - s\phi c\psi & c\phi c\theta \end{bmatrix} \underbrace{\begin{bmatrix} I \\ J \\ K \end{bmatrix}}_{Inertial\ frame} \tag{6}$$

where ϕ is the roll angle, θ is the pitch angle, and ψ is the yaw angle.

$$\begin{bmatrix} c\theta c\psi & c\theta s\psi & -s\theta \\ s\phi s\theta c\psi - c\phi s\psi & s\phi s\theta s\psi + c\phi c\psi & s\phi c\theta \\ c\phi s\theta c\psi + s\phi s\psi & c\phi s\theta s\psi - s\phi c\psi & c\phi c\theta \end{bmatrix} \begin{bmatrix} 0 \\ 0 \\ g \end{bmatrix} = \begin{bmatrix} -gs\theta \\ gs\phi c\theta \\ gc\phi c\theta \end{bmatrix} \tag{7}$$

$$m\frac{d}{dt}\left(\begin{bmatrix}u\\v\\w\end{bmatrix}\right)=\begin{bmatrix}F_x\\F_y\\F_z\end{bmatrix}-m\begin{bmatrix}-gs\theta\\gs\phi c\theta\\gc\phi c\theta\end{bmatrix}-\begin{bmatrix}p\\q\\r\end{bmatrix}\times\left(m\begin{bmatrix}u\\v\\w\end{bmatrix}\right) \tag{8}$$

$$\begin{bmatrix}\dot{u}\\\dot{v}\\\dot{w}\end{bmatrix}=\frac{1}{m}\begin{bmatrix}F_x\\F_y\\F_z\end{bmatrix}-\begin{bmatrix}-gs\theta\\gs\phi c\theta\\gc\phi c\theta\end{bmatrix}-\begin{bmatrix}qw-rv\\ru-pw\\pv-qu\end{bmatrix} \tag{9}$$

For $x-axis$

$$\dot{u}=\frac{F_x}{m}+gs\theta+rv-qw \tag{10}$$

For $y-axis$

$$\dot{v}=\frac{F_y}{m}-gc\theta s\phi+pw-ru \tag{11}$$

For $z-axis$

$$\dot{w}=\frac{F_z}{m}-gc\theta c\phi+qu-pv \tag{12}$$

3.2.2. Rotational Accelerations

Newton's second law is also applied to calculate the angular accelerations using the equation below

$$M_s=\frac{d}{dt}([I]\vec{\omega})+\vec{\omega}\times([I]\vec{\omega}) \tag{13}$$

where M_s is surface moments on the rocket body ($[L \quad M \quad N]^T$), I is the inertia matrix of the rocket.

$$[I]=\begin{bmatrix}I_{xx}&I_{xy}&I_{xz}\\I_{yx}&I_{yy}&I_{yz}\\I_{zx}&I_{zy}&I_{zz}\end{bmatrix} \tag{4}$$

The assumptions for the moment of inertia are the rocket body is symmetric along

$xz, xy, and\ yz$ planes. Therefore, Eq. 14 becomes;

$$[I] = \begin{bmatrix} I_{xx} & 0 & 0 \\ 0 & I_{yy} & 0 \\ 0 & 0 & I_{zz} \end{bmatrix} \quad (5)$$

The values of the inertia matrix obtained by the CAD model drawn by me on Fusion 360.

$$\begin{bmatrix} L \\ M \\ N \end{bmatrix} = \begin{bmatrix} I_{xx} & 0 & 0 \\ 0 & I_{yy} & 0 \\ 0 & 0 & I_{zz} \end{bmatrix} \begin{bmatrix} \dot{p} \\ \dot{q} \\ \dot{r} \end{bmatrix} + \begin{bmatrix} p \\ q \\ r \end{bmatrix} \times \begin{bmatrix} I_{xx} & 0 & 0 \\ 0 & I_{yy} & 0 \\ 0 & 0 & I_{zz} \end{bmatrix} \begin{bmatrix} p \\ q \\ r \end{bmatrix} \quad (6)$$

where $L, M\ and\ N$ are the moments on $x, y\ and\ z$ axis, respectively.

$$\begin{bmatrix} L \\ M \\ N \end{bmatrix} = \begin{bmatrix} I_{xx}\dot{p} \\ I_{yy}\dot{q} \\ I_{zz}\dot{r} \end{bmatrix} + \begin{bmatrix} p \\ q \\ r \end{bmatrix} \times \begin{bmatrix} I_{xx}p \\ I_{yy}q \\ I_{zz}r \end{bmatrix} \quad (7)$$

$$\begin{bmatrix} I_{xx}\dot{p} \\ I_{yy}\dot{q} \\ I_{zz}\dot{r} \end{bmatrix} = \begin{bmatrix} L \\ M \\ N \end{bmatrix} - \begin{bmatrix} (I_{zz} - I_{yy})qr \\ (I_{xx} - I_{zz})rp \\ (I_{yy} - I_{xx})pq \end{bmatrix} \quad (8)$$

$$\dot{p} = \frac{L}{I_{xx}} + \frac{I_{yy} - I_{zz}}{I_{xx}} qr \quad (19)$$

$$\dot{q} = \frac{M}{I_{yy}} + \frac{I_{zz} - I_{xx}}{I_{yy}} rp \quad (20)$$

$$\dot{r} = \frac{N}{I_{zz}} + \frac{I_{xx} - I_{yy}}{I_{zz}} pq \quad (21)$$

3.2.3. Kinematic Transformations

I have used Euler angles to represent the rotation of the rocket body. But this representation has a flaw that caused by the pitch angle.

$$\begin{bmatrix}\dot{\phi}\\ \dot{\theta}\\ \dot{\psi}\end{bmatrix} = \begin{bmatrix}1 & s\phi t\theta & c\phi t\theta\\ 0 & c\phi & -s\phi\\ 0 & \dfrac{s\phi}{c\theta} & \dfrac{c\phi}{c\theta}\end{bmatrix}\begin{bmatrix}p\\ q\\ r\end{bmatrix} \quad (22)$$

In the calculation of the Euler angle (can be seen above), there are some divisions by zeros. Therefore, even though I used this method as a starting point, I have switched to quaternion representation.

$$Q = \begin{bmatrix} c\frac{\phi}{2}c\frac{\theta}{2}c\frac{\psi}{2} + s\frac{\phi}{2}s\frac{\theta}{2}s\frac{\psi}{2}\\ s\frac{\phi}{2}c\frac{\theta}{2}c\frac{\psi}{2} - c\frac{\phi}{2}s\frac{\theta}{2}s\frac{\psi}{2}\\ c\frac{\phi}{2}s\frac{\theta}{2}c\frac{\psi}{2} + s\frac{\phi}{2}c\frac{\theta}{2}s\frac{\psi}{2}\\ c\frac{\phi}{2}c\frac{\theta}{2}s\frac{\psi}{2} - s\frac{\phi}{2}s\frac{\theta}{2}c\frac{\psi}{2}\end{bmatrix} \quad (23)$$

Quaternions can be used in this form. However, the quaternion needs to be normalized.

$$[\dot{Q}] = \frac{1}{2}[Q]\otimes\begin{bmatrix}0\\ p\\ q\\ r\end{bmatrix} \quad (24)$$

where $\otimes$ is the quaternion product.

The above equation can be written in a different form,

$$[\dot{Q}] = \frac{1}{2}\begin{bmatrix}0 & -p & -q & -r\\ p & 0 & r & -q\\ q & -r & 0 & p\\ r & q & -p & 0\end{bmatrix}[Q] \quad (25)$$

In order to correct the orthogonality error of the equation above, the diagonal part can be replaced by $K\epsilon$ term where K is the gain coefficient and $\epsilon = 1 - (q_0^2 + q_1^2 + q_2^2 + q_3^2)$. $K\epsilon$ term on the diagonal can be added as below;

$$\begin{bmatrix}\dot{q_0}\\ \dot{q_1}\\ \dot{q_2}\\ \dot{q_3}\end{bmatrix} = \frac{1}{2}\begin{bmatrix}0 & -p & -q & -r\\ p & 0 & r & -q\\ q & -r & 0 & p\\ r & q & -p & 0\end{bmatrix}\begin{bmatrix}q_0\\ q_1\\ q_2\\ q_3\end{bmatrix} + K\epsilon\begin{bmatrix}q_0\\ q_1\\ q_2\\ q_3\end{bmatrix} \tag{9}$$

3.2.4. Thrust Vector Forces and Moments

The gimbal on the rocket rotates in axis. They are $y\ and\ z$ axis. To calculate the vector components of the thrust rotation matrix can be used.

$$\begin{bmatrix}T_x\\ T_y\\ T_z\end{bmatrix} = R_y(\lambda)R_z(\mu)\begin{bmatrix}T\\ 0\\ 0\end{bmatrix} \tag{10}$$

Where $R_y(\lambda)$ is the rotation matrix by the angle of λ on y axis, $R_z(\mu)$ is the rotation matrix by the angle of μ on z axis, $T_x, T_y, and\ T_z$ are the thrust components on $x, y, and\ z$ axis, respectively.

$$\begin{bmatrix}T_x\\ T_y\\ T_z\end{bmatrix} = \begin{bmatrix}Tc\lambda c\mu\\ Ts\mu\\ -Ts\lambda c\mu\end{bmatrix} \tag{11}$$

These thrust components also create moments since there is a distance between gimbal centre to centre of gravity of the rocket on the x axis. That's why the moments need to be taken into account.

$$M_{t,y} = T_z * d_{TVC-CG} \tag{29}$$

$$M_{t,z} = T_y * d_{TVC-CG} \tag{12}$$

3.2.5. Aerodynamics

The drag force acts on the centre of pressure and it is parallel and opposite to velocity vector of the rocket. Since the drag is in the wind frame, some transformation needed to be done.

$$[F_{A,w}] = \begin{bmatrix} F_{Ax,w} \\ F_{Ay,w} \\ F_{Az,w} \end{bmatrix} = \begin{bmatrix} -0.5\rho V^2 S C_A \\ -0.5\rho V^2 S C_{N,y} \\ -0.5\rho V^2 S C_{N,z} \end{bmatrix} \tag{13}$$

where ρ is the atmospheric density, V is the magnitude of the velocity vector of the rocket, S is the reference area, C_A is the axial force coefficient, C_N is the normal force coefficient, $C_{N,y}$ is the normal force coefficient on yb-axis, $C_{N,z}$ is the normal force coefficient on zb-axis.

$$C_{N,y} = C_N \frac{-v}{\sqrt{v^2 + w^2}} \tag{14}$$

$$C_{N,z} = C_N \frac{1}{\sqrt{v^2 + w^2}} \tag{15}$$

Calculation of aerodynamic coefficients is not covered in this study. Coefficients are obtained from related works.

$$[F_{A,b}] = \begin{bmatrix} c\alpha c\beta & -c\alpha s\beta & -s\alpha \\ s\beta & c\beta & 0 \\ s\alpha c\beta & -s\alpha s\beta & c\alpha \end{bmatrix} \begin{bmatrix} -0.5\rho V^2 S C_A \\ -0.5\rho V^2 S C_{N,y} \\ -0.5\rho V^2 S C_{N,z} \end{bmatrix} \tag{16}$$

$$\begin{bmatrix} L_A \\ M_A \\ N_A \end{bmatrix} = \begin{bmatrix} 0 \\ 0.5\rho V^2 S d_{CG-CP} C_{N,z} \\ 0.5\rho V^2 S d_{CG-CP} C_{N,y} \end{bmatrix} \tag{17}$$

where d_{CG-CP} is the distance between the C_P and C_G, $L_A, M_A, and\ N_A$ is the aerodynamics moments on $x, y, and\ z$-axis, respectively [11].

4. CAD MODEL

Several designs for TVC gimbals have been examined. Many gimbals usually attached directly to the rocket motor or a casing that holds the motor. Most of them uses two servos, one for y-axis and one for z-axis. The servos used in these gimbals are fairly low budget, simple and light-weight servos such as SG90 [12]. These servos rotate the motor casing or the motor using a piece of wire that is connected to the plastic extension of the gimbal and the servo's blade on two axes. Another design that has been examined is the design of T-Zero Systems and it can be seen in Fig. 4.1. This design is unique than any other design because it uses rubbery plastic hinge in the between of thrust reaction structure and the engine mount. This gives the structure to be compliant. It uses two servos that is connected to the engine mount by two integrated linkage to rotate the engine in two axes.

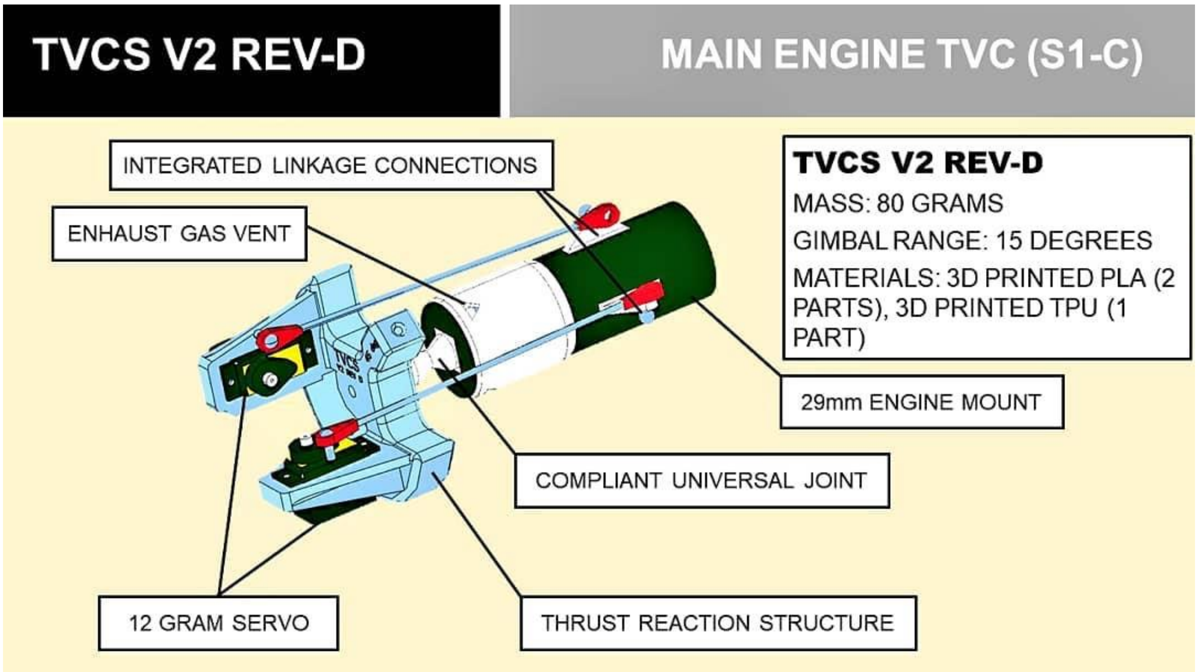

Figure 4.1 T-Zero Systems' complaint TVC gimbal design [13]

On my design, I will use the most common design and this design can be seen in Fig. 4.2.

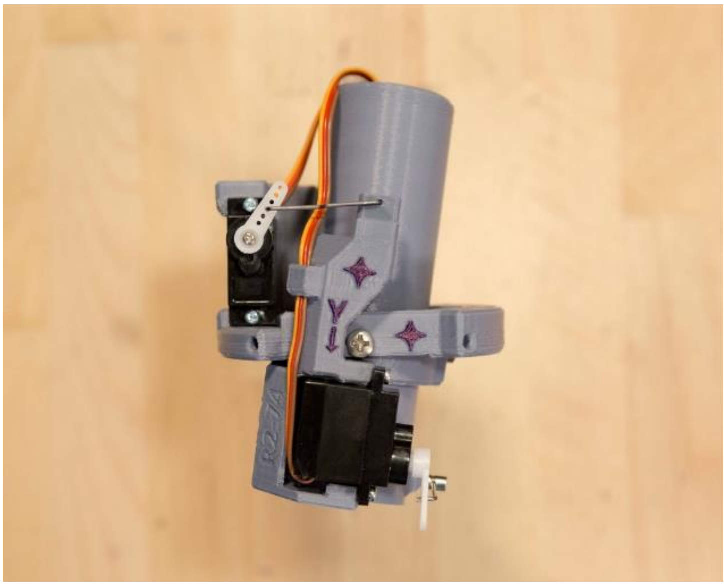

Figure 4.2 Most common design for TVC gimbals [14]

This will provide me handful of different designs. I have used Fusion 360 to design the CAD model of my TVC gimbal. I have started with ballpark measurements for the gimbal. The motor casing was the first modelling done. After that inner piece of the gimbal got modelled. As a last thing the outer piece got modelled. A servo similar to SG90 also modelled in a simple manner as an accessory. For the rocket body, a simple hollow cylinder has been modelled. For the nose cone, ogive shape has been used. The shape created by using the profile in Fig. 4.3 [15]. The complete design of the gimbal can be seen in Fig. 4.4.

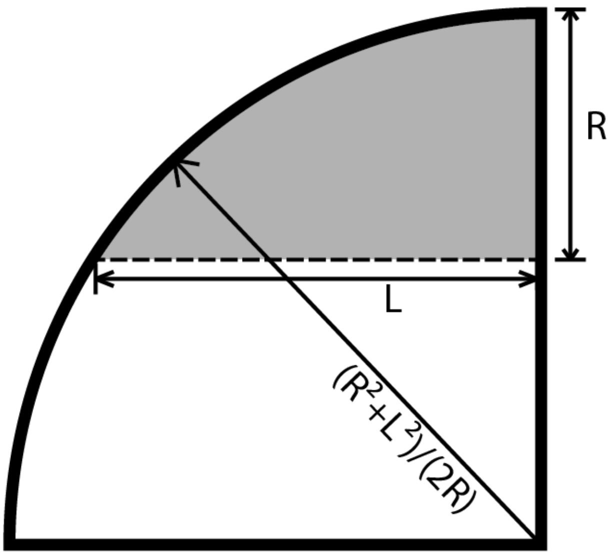

Figure 4.3 The ogive nose cone profile

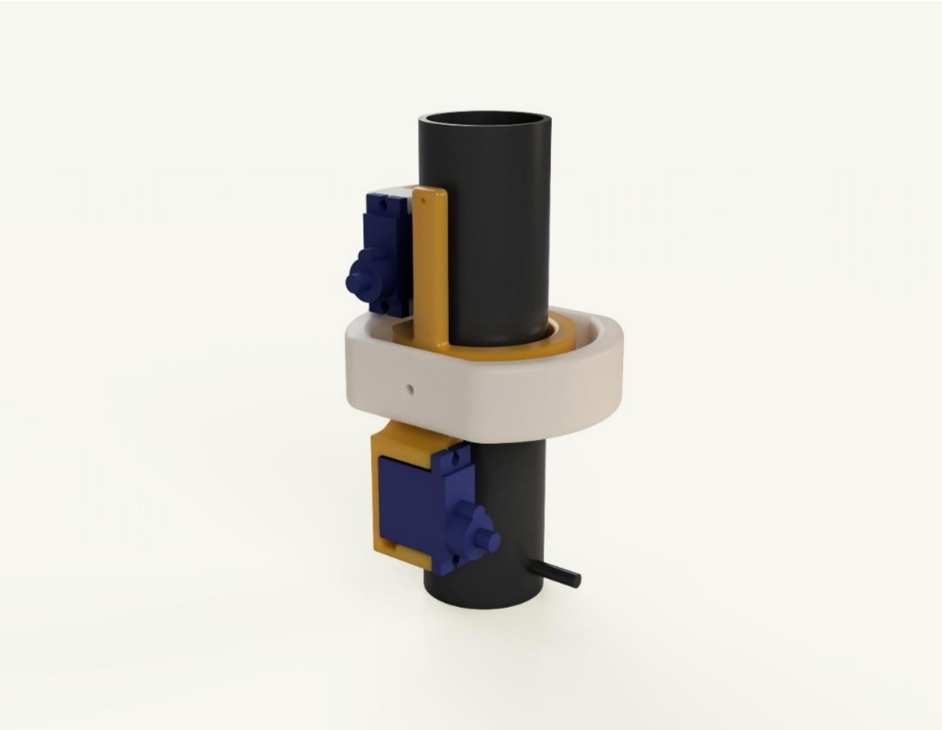

Figure 4.4 My design for TVC gimbal

The materials, mass information of the parts can be found in the Table 4.1. The dimension and the blueprints of the parts can be found in the Appendix section.

Table 4.1 The materials and mass information of the parts

#	Part Name	Material	Mass (grams)
1	Nose Cone	ABS Plastic	200.309
2	Body Tube	ABS Plastic	704.913
3	Outer Ring Gimbal	PA 11 - Nylon- HP 11-30	35.477
4	Outer Ring Servo	Laminate	9.969
5	Inner Ring Gimbal	PA 11 - Nylon- HP 11-30	24.684
6	Inner Ring Servo	Laminate	9.969
7	Motor Tube	PVC Piping	36.787
		$\sum mass$	1012.109

The moment of inertia as well as the centre of gravity location got calculated by Fusion 360 with the CAD model that had been designed. Also for the location of the centre of pressure, an open source rocket design simulation software called OpenRocket has been used. Even though there wasn't a feature to import my CAD model to OpenRocket, a similar rocket has been designed based on the nose cone, the body tube and the location of the C_G on the Fusion 360. The material or the mass distribution of the parts doesn't affect the location of C_P except aerodynamic shape like nose cone design and fins. Since the model had no fins and the software had the exact nose cone design I had used, the location information for C_P was accurate enough. The information regarding these can be found Table 4.2. All the location information on this table is measured from the bottom of the rocket tube.

Table 4.2 Moment of inertias, $\boldsymbol{C_G}$ and $\boldsymbol{C_P}$ location information

	Rocket Assembly
Centre of Gravity	$509.023\ mm$
Centre of Pressure	$1061.00\ mm$
I_{xx}	$1.384 * 10^6\ g \cdot mm$^2
I_{yy}	$1.205 * 10^8\ g \cdot mm$^2
I_{zz}	$1.205 * 10^8\ g \cdot mm$^2

Figure 4.5 Full assembly of the rocket

5. SIMULINK MODEL

5.1. Dynamics Part

The translational acceleration of x-axis of the rocket found on Eq. 10. Hence, the model was formed accordingly.

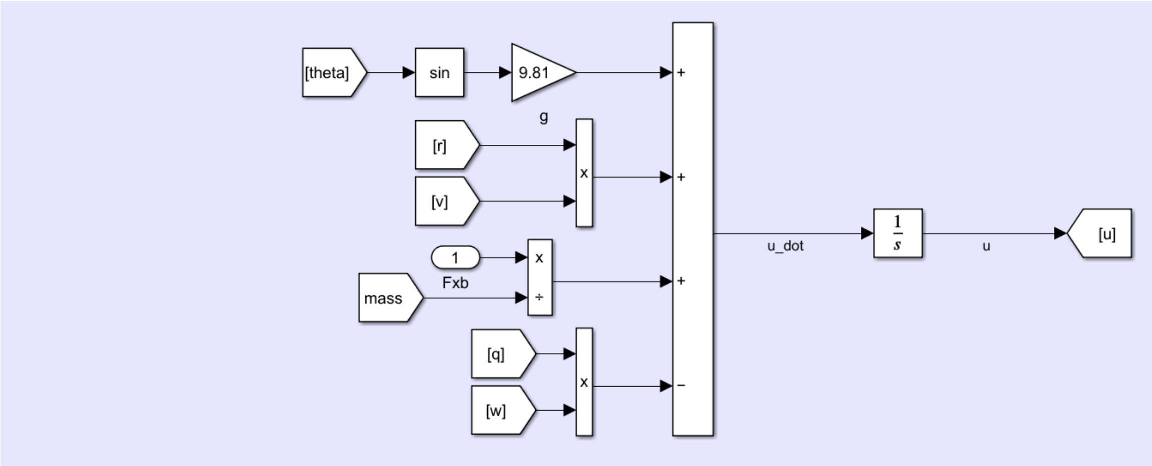

Figure 5.1.1 Translational acceleration and velocity model for x-axis

The translational acceleration of y-axis was formed using Eq. 11.

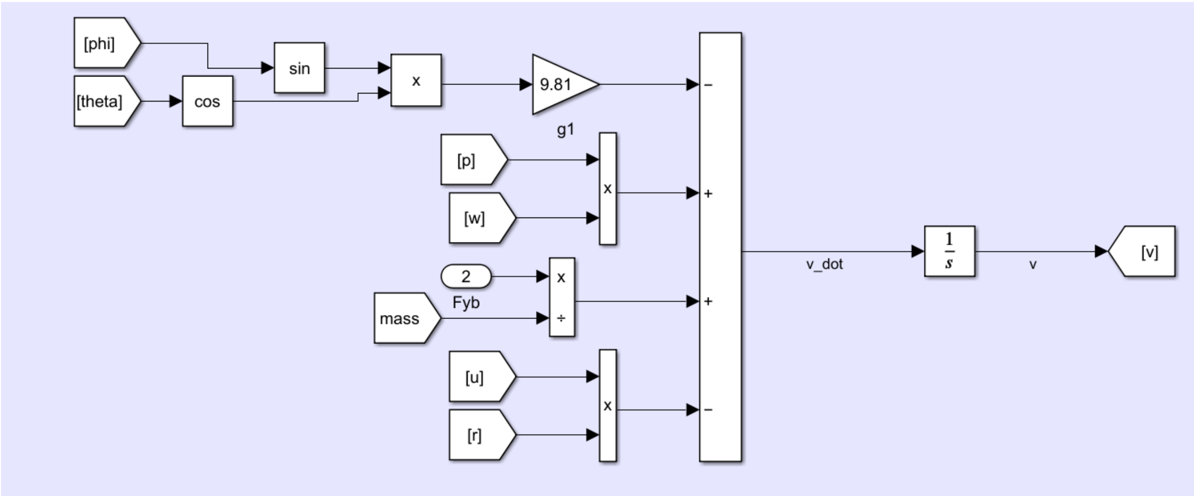

Figure 5.1.2 Translational acceleration and velocity model for y-axis

The translational acceleration of z-axis was formed using Eq. 12.

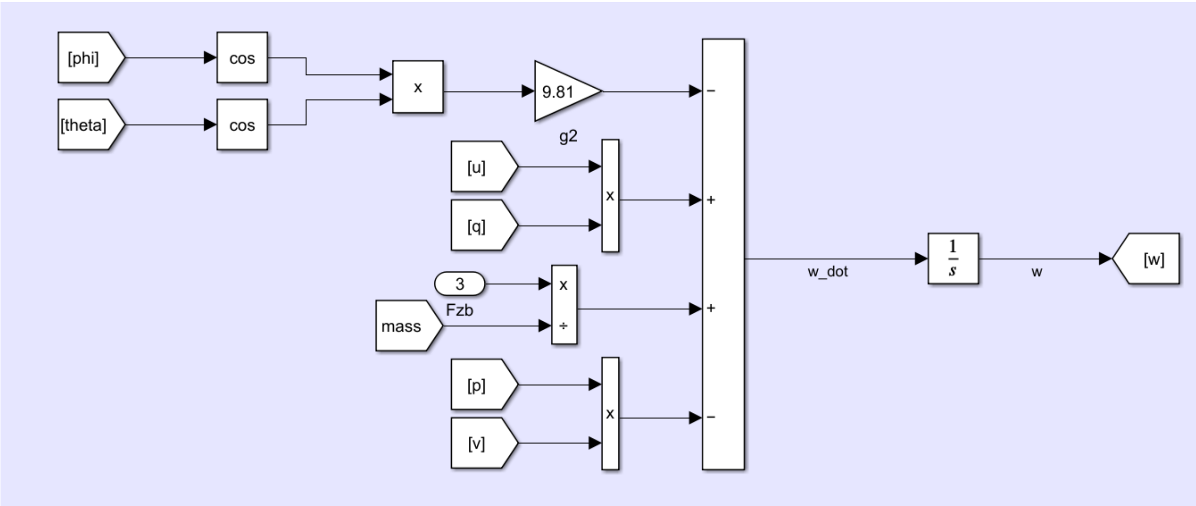

Figure 5.1.3 Translational acceleration and velocity model for z-axis

Using an integrator block on all the acceleration terms $u, v, and\ w$ are obtained. The initial conditions of these velocities are all the same and equal to zero.

The model for angular acceleration on x-axis, $\dot{p}$, was formed using Eq. 19.

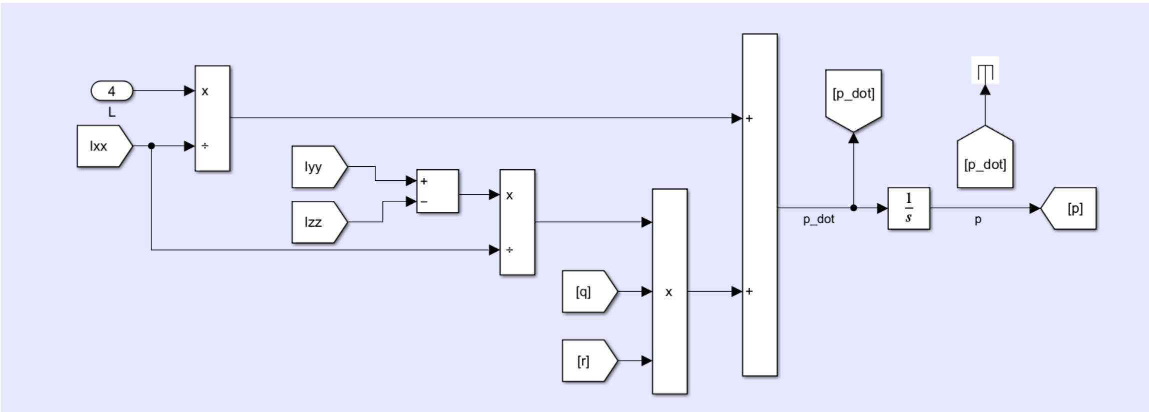

Figure 5.1.4 Angular acceleration and velocity model for x-axis

The model for angular acceleration on y-axis, $\dot{q}$, was formed using Eq. 20.

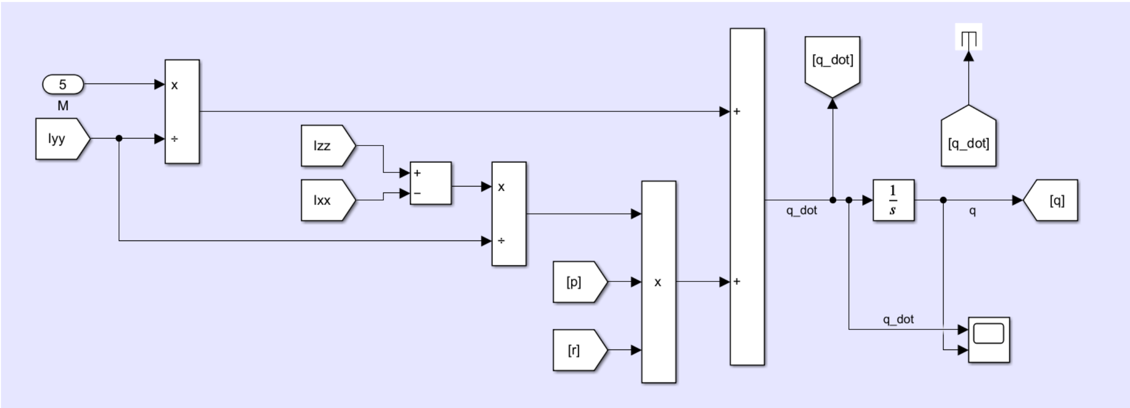

Figure 5.1.5 Angular acceleration and velocity model for y-axis

The model for angular acceleration on z-axis, $\dot{r}$, was formed using Eq. 21.

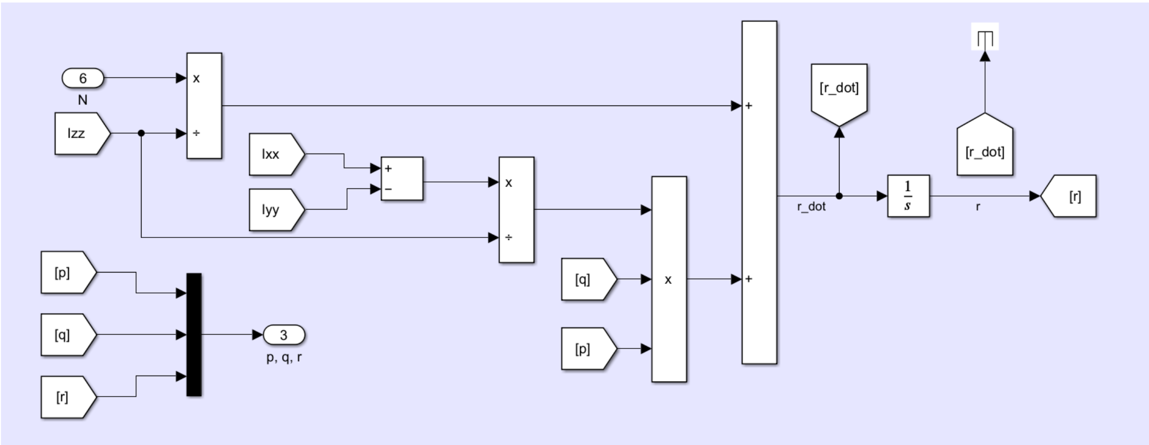

Figure 5.1.6 Angular acceleration and velocity model for z-axis

Using an integrator block on all the acceleration terms $p, q, and\ r$ are obtained. The initial conditions of these velocities are all the same and equal to zero.

The initial conditions like moment of inertias, mass, and Euler angles are created by using constant blocks. To avoid the messy signals, global goto blocks have been used. Hence, the values can be changed without opening a subsystem.

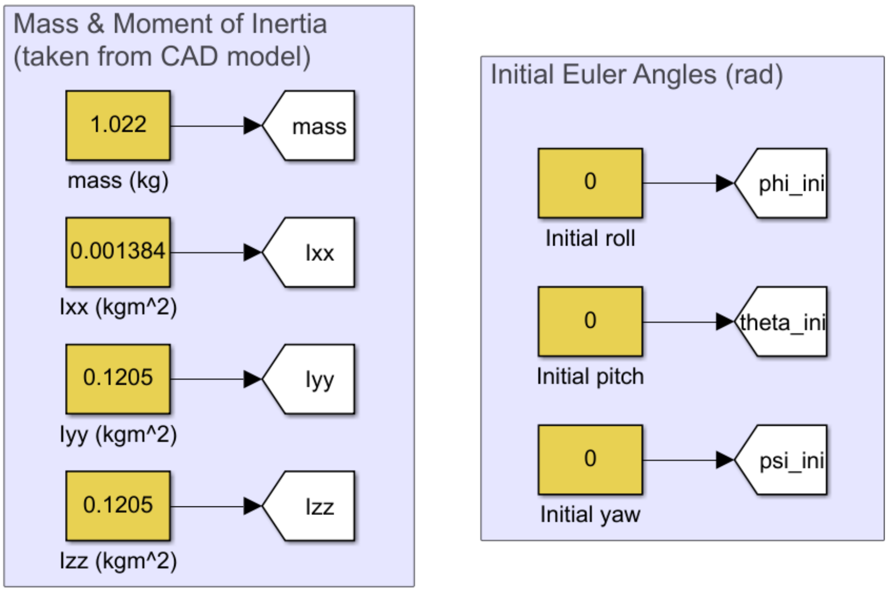

Figure 5.1.7 Mass (kg), moment of inertias (kgm^2) and initial Euler angles (rad) inputs

The modelling for quaternions and Euler angles were formed by using Eq. 26. For the start of the simulation, an initial rotation has been set and can be seen above. This gave the system to initial quaternion values by using an integrator with external initial conditions. Obtained quaternion vector get transformed into a direct cosine matrix in order to obtain earth frame translational velocities ($\dot{X}_e, \dot{Y}_e, and\ \dot{Z}_e$). With that values, the position values in the earth frame have been obtained using an integrator. Also, with the quaternion matrix, Euler angles has been calculated to use them in the *6DOF animation*.

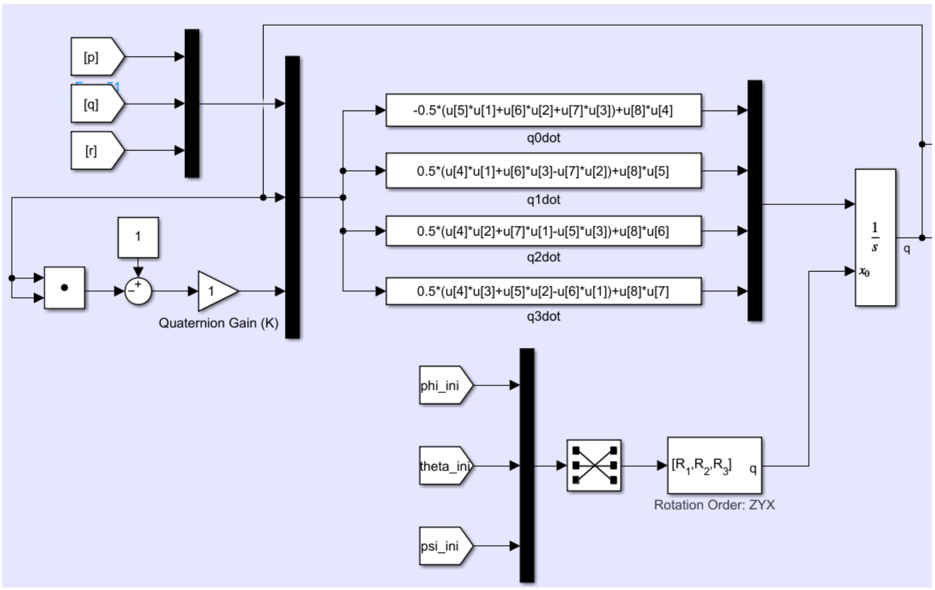

Figure 5.1.8 Quaternion matrix calculation model

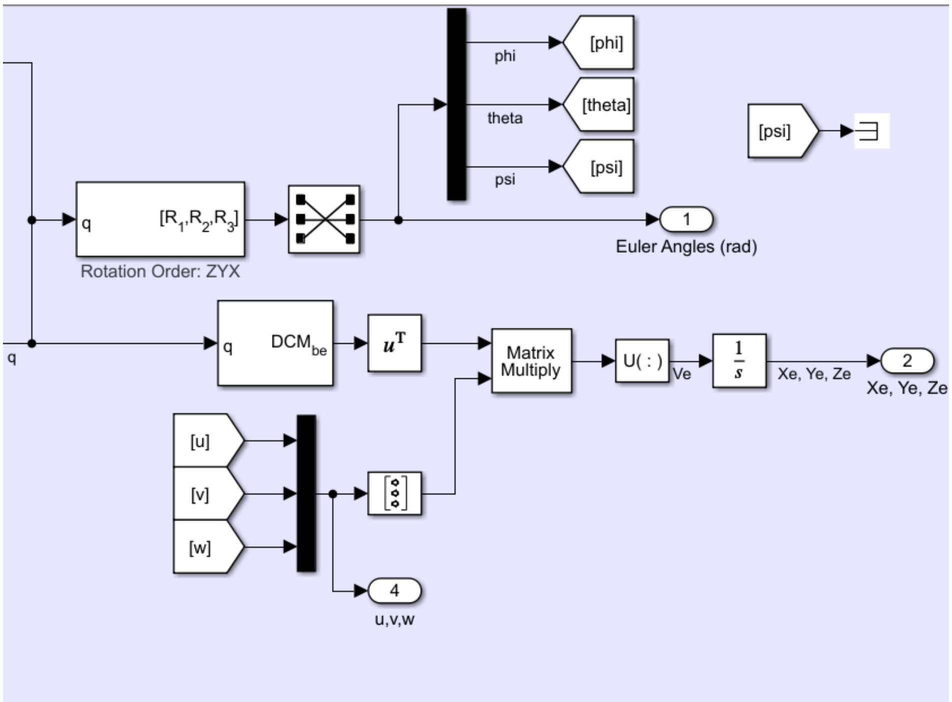

Figure 5.1.9 Euler angles and Earth frame transformation using quaternions model

The model of the thrust vector components and moments were formed using Eq. 29. The input thrust modelled as constant 100 Newtons for the simplicity by using a signal builder block.

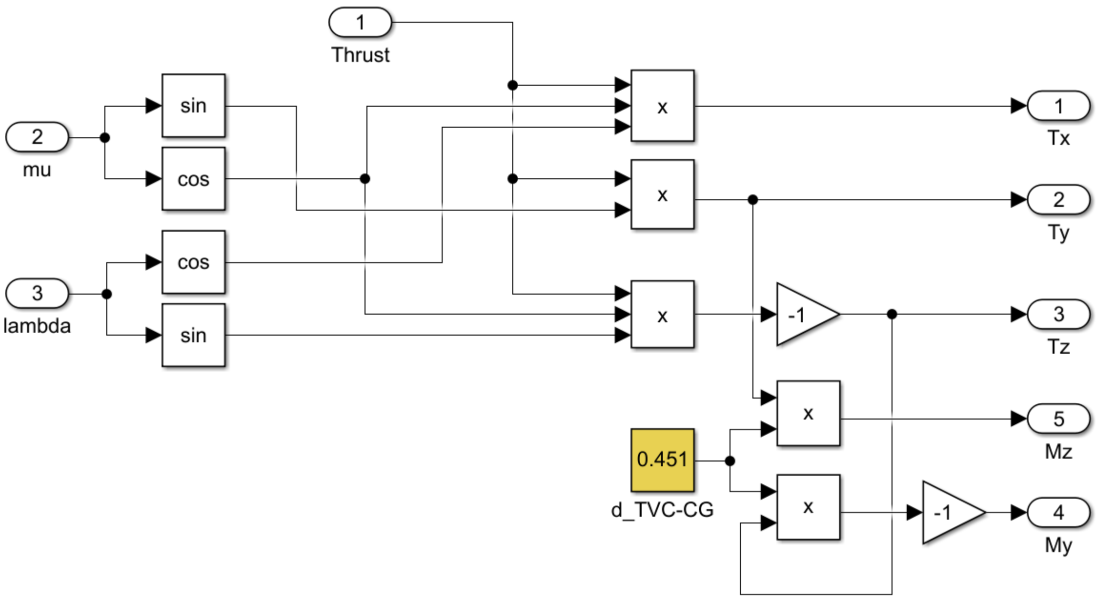

Figure 5.1.10 Thrust vector force and moment components

The distance between thrust vector gimbal's centre of mass and centre of gravity of the rocket has been measured in Fusion 360.

For the animation, *6DoF Animation* block from *Aerospace Blockset* has been used. This block uses a pre-written MATLAB function and the positive z-axis acts downward in this animation. In order to change that effect, the position value on the Z-axis of the earth frame has been multiplied by -1. In addition to that, a simple stop simulation condition added to prevent the rocket going underground. Also, for the calculation of ρ and mach number, altitude value (position on the Z-axis of the earth frame) taken as output without any change on the value. Since the initial condition for Euler angles are zero, the rocket goes sideways on the animation. To correct this behaviour, rather than writing a new animation function a 90° correction angle added to roll angle.

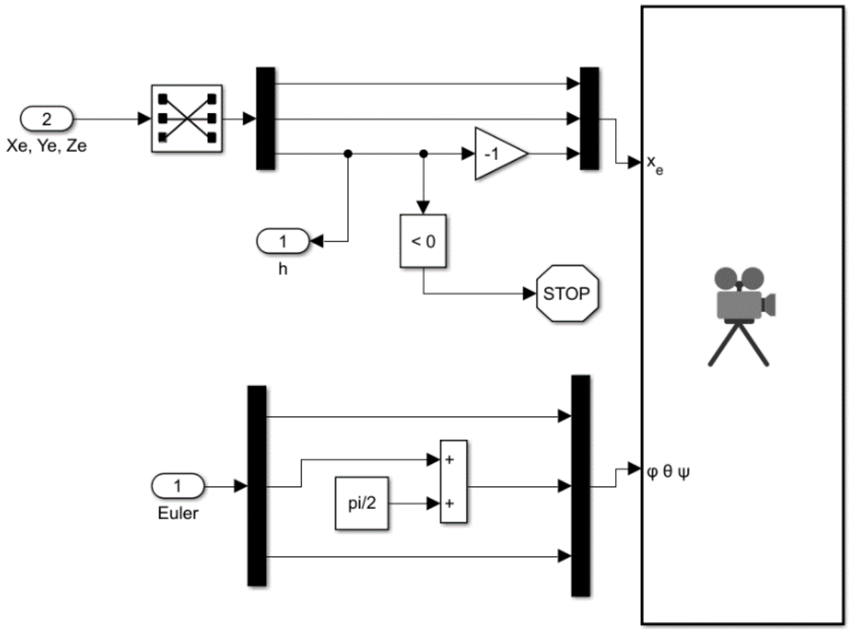

Figure 5.1.11 Animation subsystem

Since the drag force acts on another frame called wind frame, it needed to transformed into body frame. The angles for this transformation comes from incidence (α) and sideslip (β) angles. The transformation matrix has been obtained in Eq. 34.

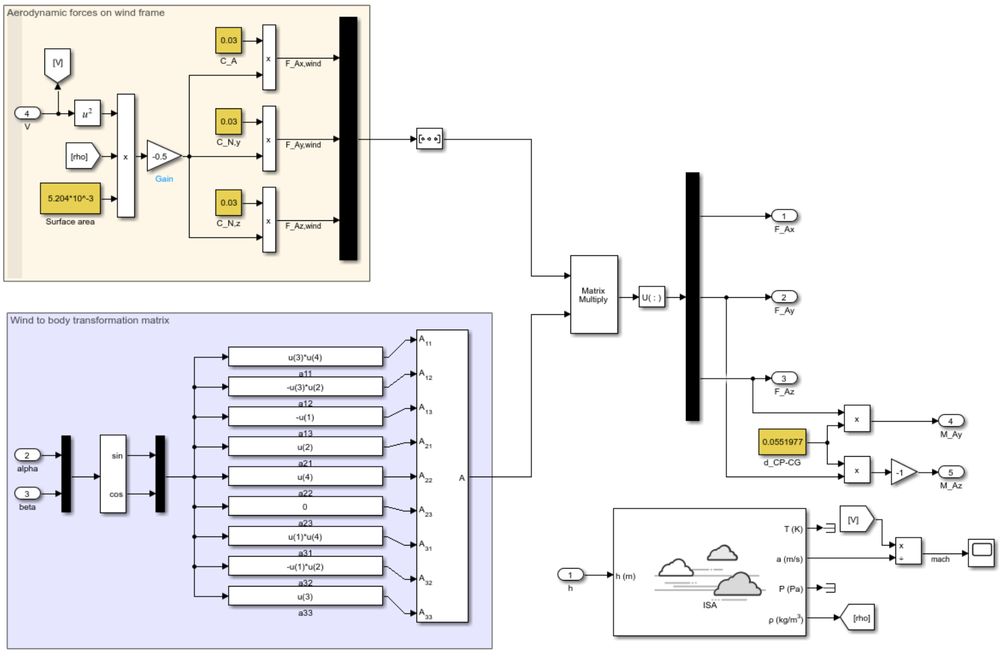

Figure 5.1.12 Aerodynamics subsystem

5.2. Control Part

The control mechanism takes place by creating side forces by rotating the gimbal to a specific angles. These side forces creates moments about the C_G of the rocket and with the help of these moments created by the gimbal, the external moments acts on the body, (in these case aerodynamic moments) aimed to cancel each other for a vertical flight. To achieve this goal, two sets of PID has been utilized, one for pitch angle and one for yaw angle. The roll angle cannot controlled with this gimbal due to lack of a way to create a moment on x-axis. For the PID, an error signal that calculates the difference between the current attitude angle value and set point angle value, which is 0 for the both angle has been used as input. The PID block for the both axis has output saturation feature since the gimbal has physical constraints on rotating. This value taken as $-5°$ to $5°$ (-0.08727 rad to 0.08727 rad) according to CAD model of the gimbal. This saturation avoided some absurd PID outputs such as rotating the gimbal upside down and made the simulation a bit realistic. As another control constraint, the gimbal creates a limited moment since the angle of rotation is limited between $-5°$ to $5°$. Therefore, there is a limit that this system can control compare to disturbance on moments. PID gains selected by trial and error method. The current gains are 8, 5, 3.2 for P, I, D, respectively.

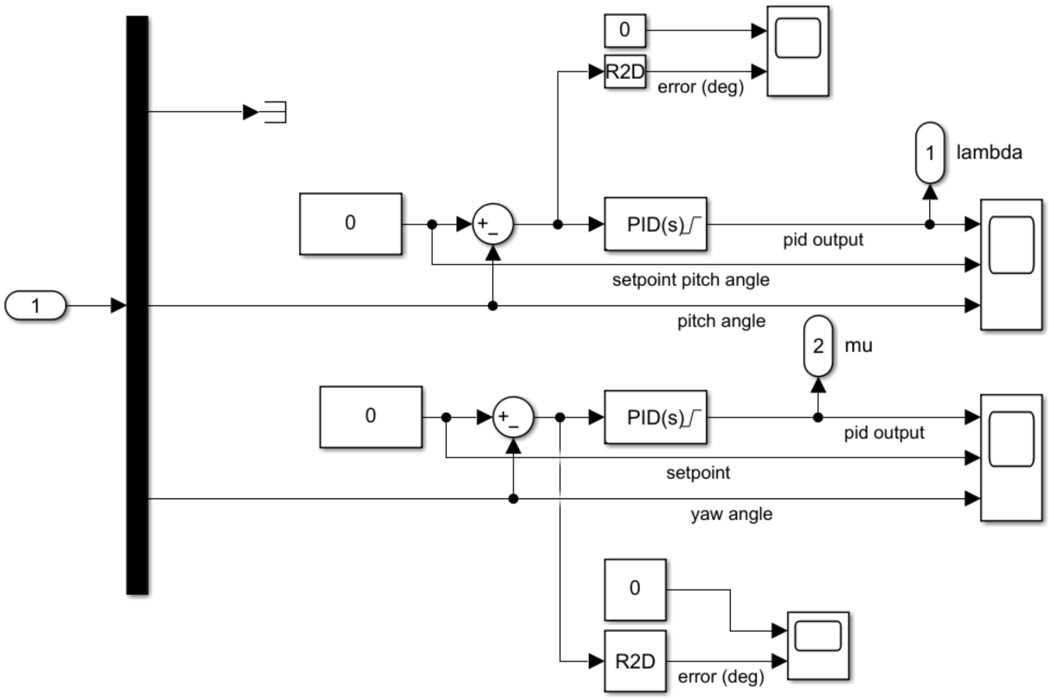

Figure 5.2.1 Control subsystem

5.3. Result

In this study, 6DOF rocket modelled. Since the rocket is naturally unstable due to lack of fins, it is controlled using 2DOF TVC gimbal. The model compared with Simulink's Aerospace Blockset in various times to check the validity of the model. The uncontrolled flight's Euler angles can be seen in Fig. 5.3.1. For the uncontrolled flight, the gimbal fixed in the natural position of zero rotation. This caused the rocket to behave unstable due to aerodynamic forces acting on the rocket body all alone.

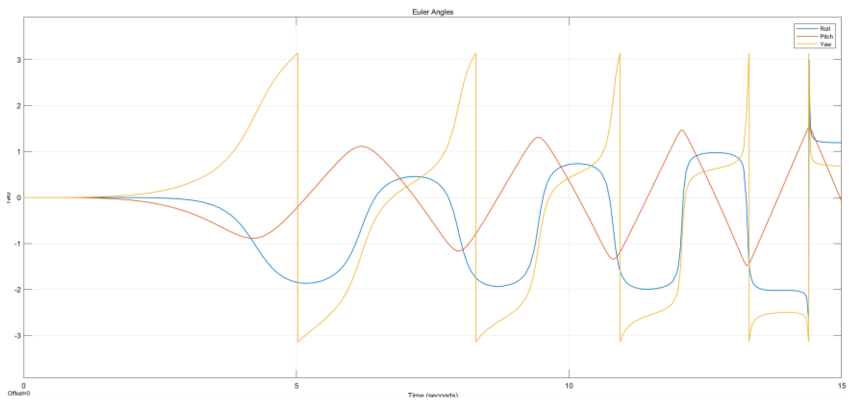

Figure 5.3.1 Euler angles for uncontrolled flight simulation

For the controlled simulation, a constant thrust of 100 Newtons has been used. The PID output signal for pitch angle and the pitch angle itself can be seen in Fig. 5.3.2. The error for pitch angle is about 0.01° at maximum which is pretty low. As another note, the PID output is also pretty low. This means the system has a potential to correct for even more disturbance applied to it.

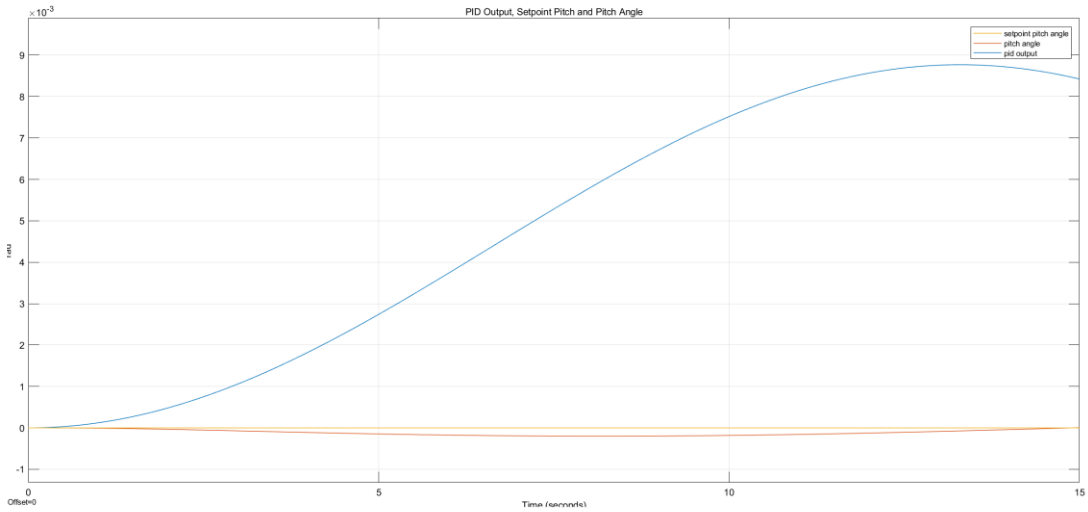

Figure 5.3.2 PID output for pitch angle vs pitch angle

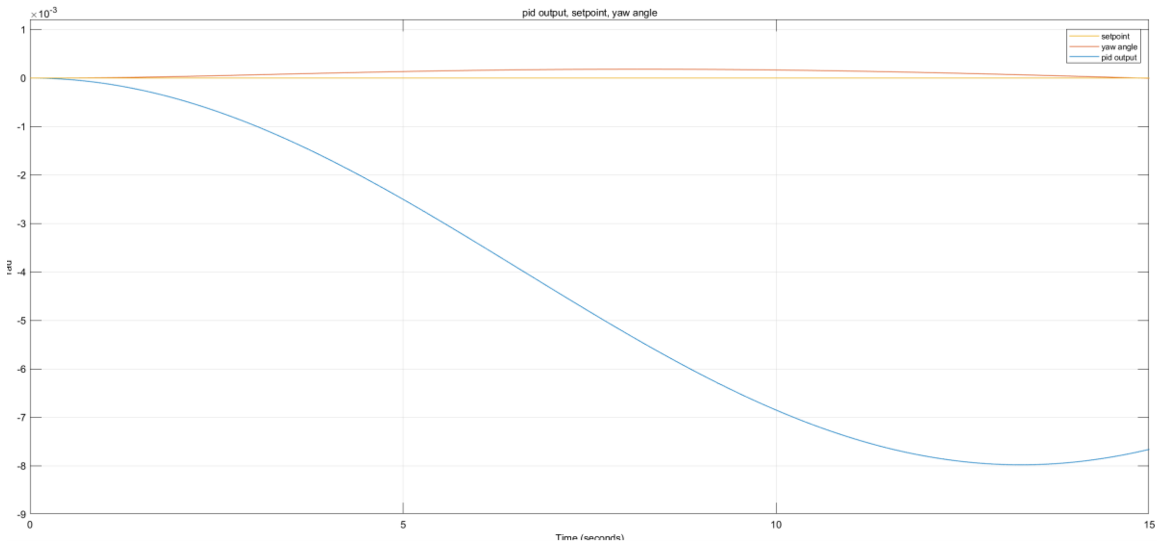

Figure 5.3.3 PID output for yaw angle vs yaw angle

The reason for the Fig. 5.3.2 and 5.3.3 are looking similar is the aerodynamics coefficient equation written in Eq. 14 and 15. When these equations used for the calculation of the aerodynamic forces as in Fig. 5.3.4, the resultant aerodynamic force on y-axis is 0 as can be seen in Fig 5.3.5. To avoid the division by zero, a simple switch block has been used.

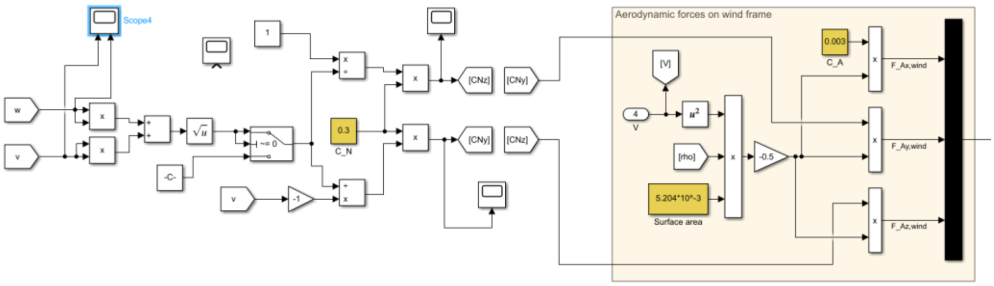

Figure 5.3.4 Aerodynamic coefficient calculation according to Eq. 14 and 15

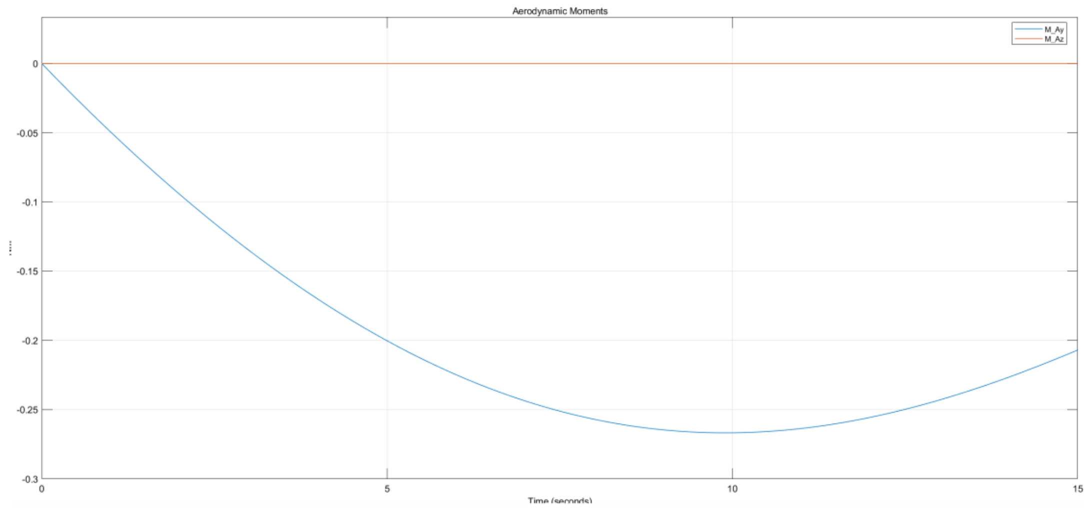

Figure 5.3.5 Aerodynamic moments for the $F_{Ay} = 0$

This is due to the initial linear velocities being equal to zero. This also causes to the aerodynamic moment on z-axis that created by aerodynamic force on y-axis to be 0. Without the disturbance the controller doesn't create any correction angle for that axis. This leads to no side force for that axis. Hence, the linear velocity being constant and 0. Therefore, a constant aerodynamic coefficient of 0.003 has been used for all axis. This resulted in same amount of moment on both axis but with a opposite sign. And gave the result that can be seen in Fig. 5.3.2 and 5.3.3. However, as another attempt to fix this problem, the initial linear velocities set to 1. This removed the division by zero problem and also created a moment for the z-axis as can be seen in Fig. 5.3.6.

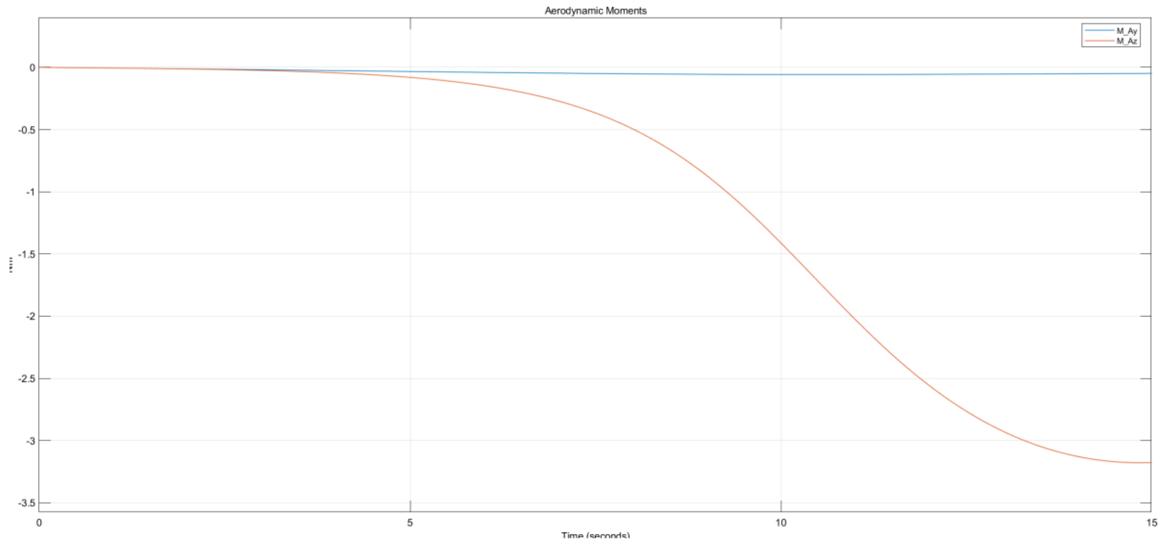

Figure 5.3.6 Aerodynamic moments with initial linear velocities of 1

With this modification, the model got better. The pitch angle control output can be seen in Fig. 5.3.7 and the yaw angle control output can be seen in Fig. 5.3.8.

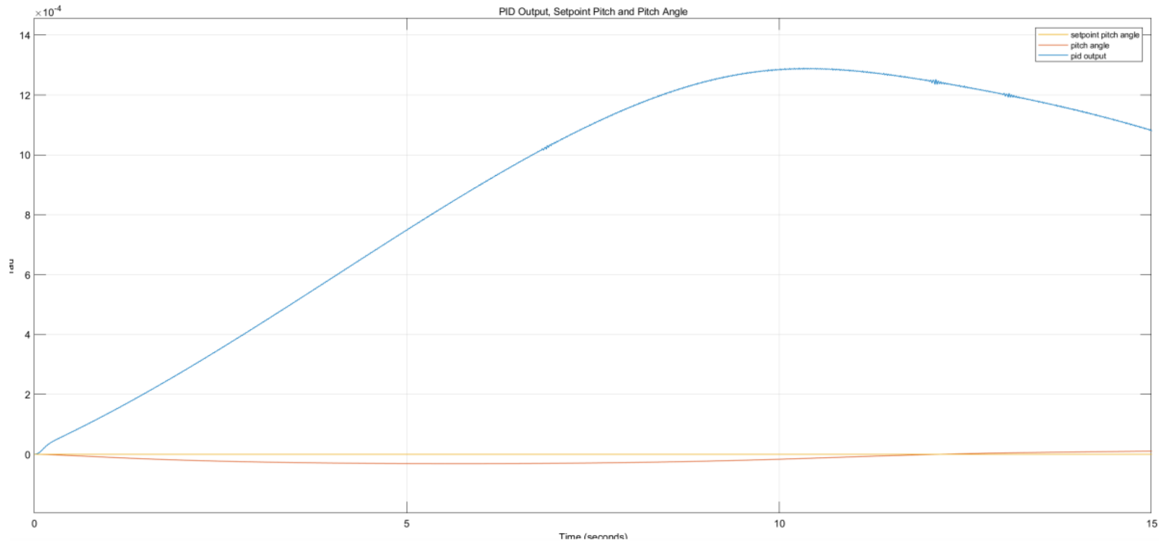

Figure 5.3.7 Pitch angle control outputs for the modified aerodynamics calculation

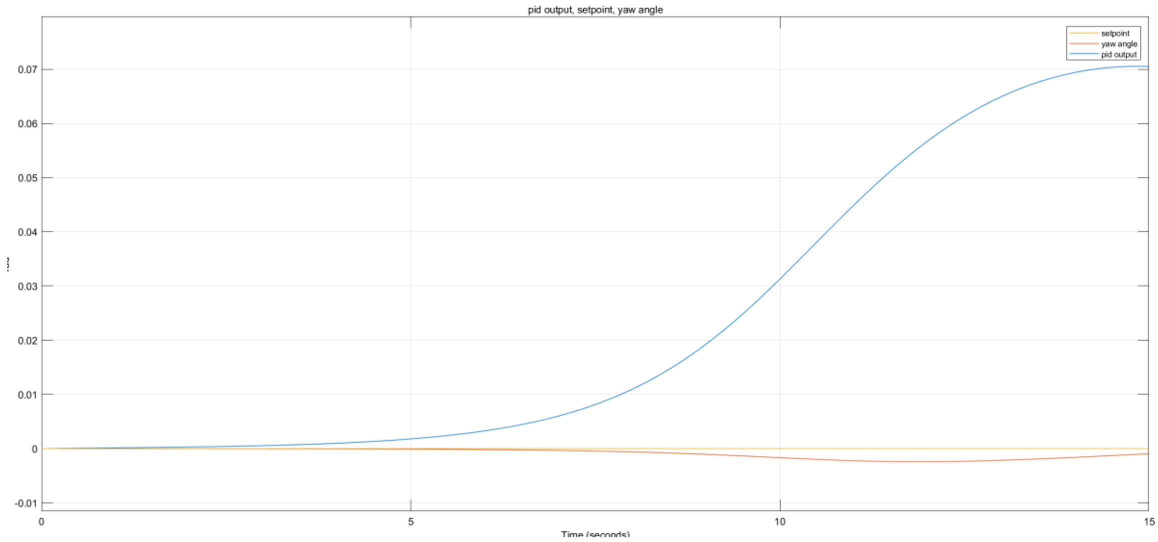

Figure 5.3.8 Yaw angle control outputs for the modified aerodynamics calculation

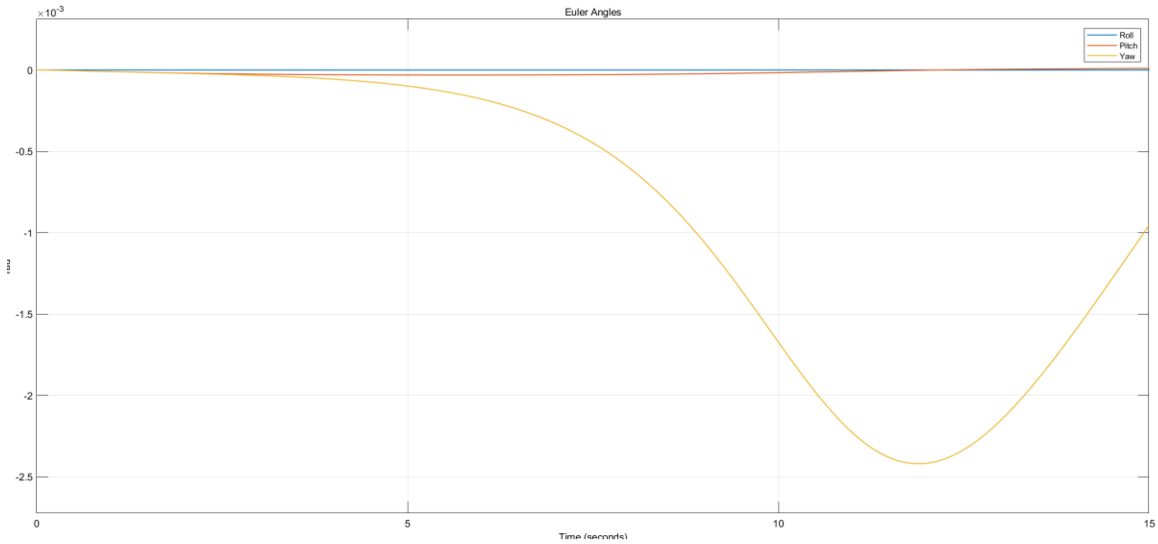

Figure 5.3.9 Euler angles for the modified aerodynamics calculation

The results of the modified aerodynamics can be get better by tuning the PID even more because the PID gains have not been changed for the modified aerodynamics calculation. However, the results are reasonable and good enough.

6. CONCLUSION

The majority of scientific operations are built on mathematical models. The study's results showed it seems reasonable to conclude that the control of the pitch and yaw angle of a 6DOF rocket without fins is possible using 2DOF gimbal attached to rocket's solid motor in the stablished limits. However, in this study, there were a couple of assumptions. That's being said, there is still much room for improvement. Such as the location C_P changes according to angle of attack, better set of data can be obtained for drag coefficients through experiments or CFD, the gimbal actuation can be modelled for more realistic simulation, other types of disturbances like gust, turbulence can be added.

REFERENCES

[1] Bibring, JP., Rosenbauer, H., Boehnhardt, H. et al. The Rosetta Lander (“Philae”) Investigations. Space Sci Rev 128, 205–220 (2007). https://doi.org/10.1007/s11214-006-9138-2

[2] Bonfiglio EP, Adams D, Craig L, Spencer D, Arvidson R, Heet T. 2011. Landing-site dispersion analysis and statistical assessment for the Mars Phoenix lander. Journal of Spacecraft and Rockets 48(5):784–797.

[3] Golombek M, Cook RA, Economou T, Folkner WM, Haldemann AFC, Kallemeyn PH, Knudsen JM, Manning RM, Moore HJ, Parker TJ, and 4 others. 1997. Overview of the Mars Pathfinder mission and assessment of landing site predictions. Science 278(5344):1743 -1748.

[4] George P. Sutton, Oscar Biblarz, Rocket Propulsion Elements, 7th Edition.

[5] R. ZEAMER. "Thrust vector control by liquid injection for solid propellant rockets," AIAA 1975-1225. 11th Propulsion Conference. September 1975.

[6] MIKE PATZER and ROBERT WHITE. "The commercial Atlas today," AIAA 1990-2715. 26th Joint Propulsion Conference. July 1990.

[7] Ankrum, T.S. (2000), 2.6.1 Germany's V-2 Rocket Program and the Application of Systems Engineering. INCOSE International Symposium, 10: 735-742. https://doi.org/10.1002/j.2334-5837.2000.tb00449.x

[8] Kalange, M. and Alcott, R., "Saturn V S-IC Stage Engine Gimbal Actuation System," SAE Technical Paper 650304, 1965, https://doi.org/10.4271/650304.

[9] Barrowman, J., 1970. Calculating the center of pressure of a model rocket. Centuri Engineering Company.

[10] Gomez, Faustino & Miikkulainen, Risto. (2003). Active Guidance for a Finless Rocket Using Neuroevolution. Lecture Notes in Computer Science. 2724. 10.1007/3-540-45110-2_105.

[11] Zanatta, Rodrigo, and Marcelo Santiago de Sousa. "A 6-DOF ROCKET MODEL FOR CONTROL ANALYSIS." International Journal of Engineering 1.1 (2015): 1-6.

[12] https://www.robotistan.com/tower-pro-sg90-rc-mini-servo-motor-eng

[13] https://runrmc94.wixsite.com/t-zero/thrust-vector-contol

[14] https://en.wikipedia.org/wiki/Nose_cone_design

[15] https://bps.space/tvc

APPENDICES

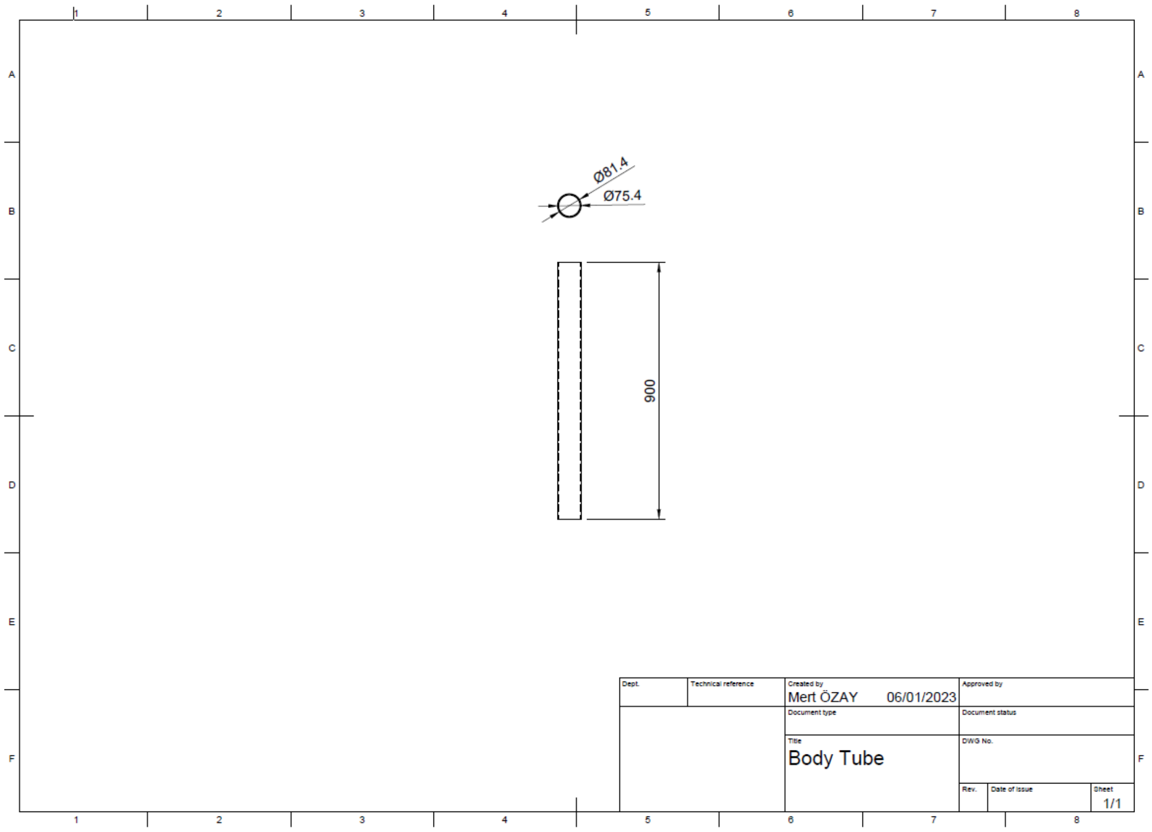

Ø81.4
Ø75.4
900
Dept.
Technical reference
Created by
Mert ÖZAY 06/01/2023
Approved by
Document type
Document status
Title
Body Tube
DWG No.
Rev.
Date of issue
Sheet
1/1

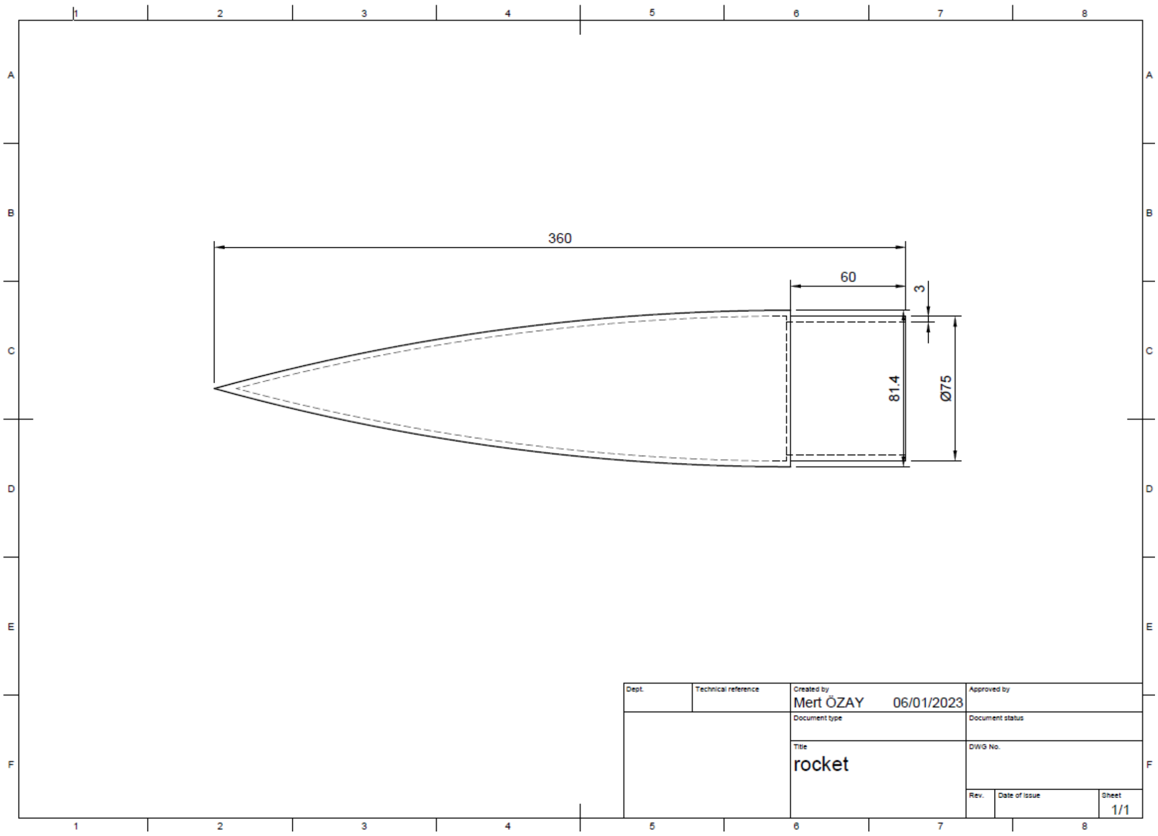

360
60
3
81.4
Ø75
Dept.
Technical reference
Created by
Mert ÖZAY 06/01/2023
Approved by
Document type
Document status
Title
rocket
DWG No.
Rev.
Date of issue
Sheet
1/1

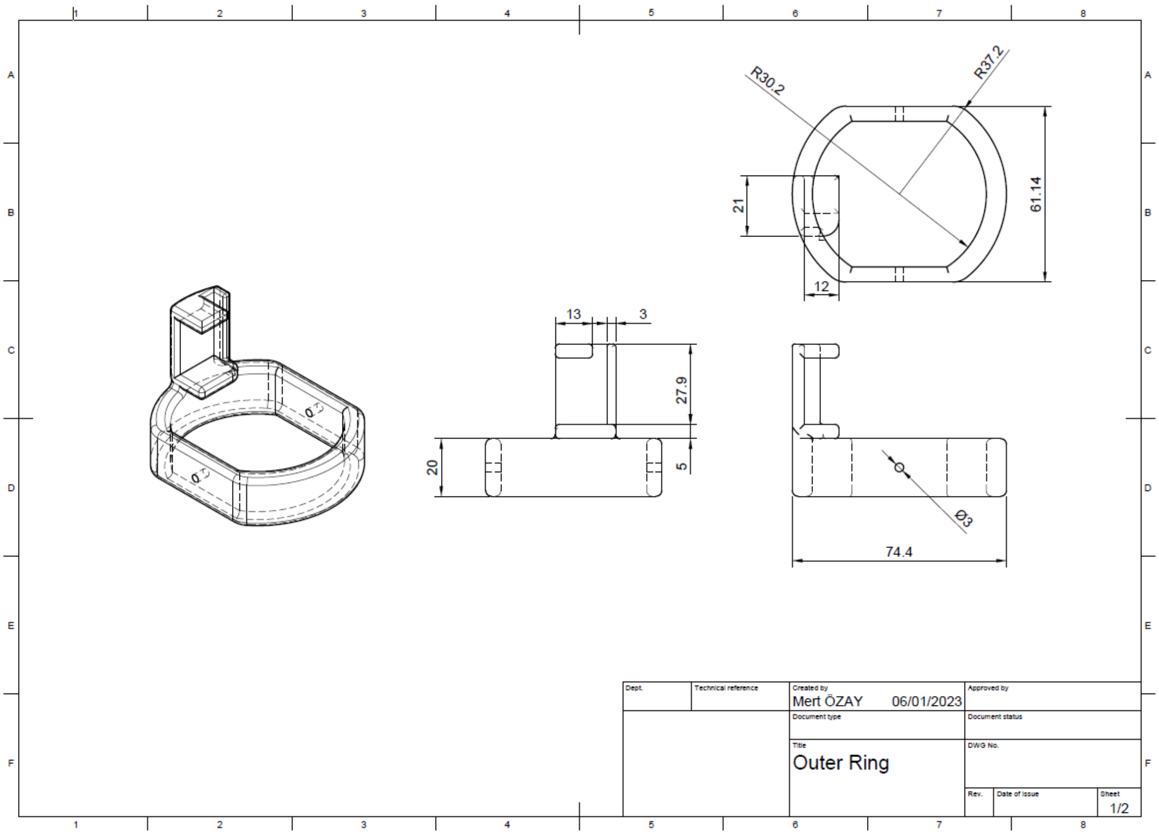
R30.2
R37.2
21
61.14
12
13
3
27.9
20
5
Ø3
74.4
Dept.
Technical reference
Created by
Mert ÖZAY 06/01/2023
Approved by
Document type
Document status
Title
Outer Ring
DWG No.
Rev.
Date of issue
Sheet
1/2

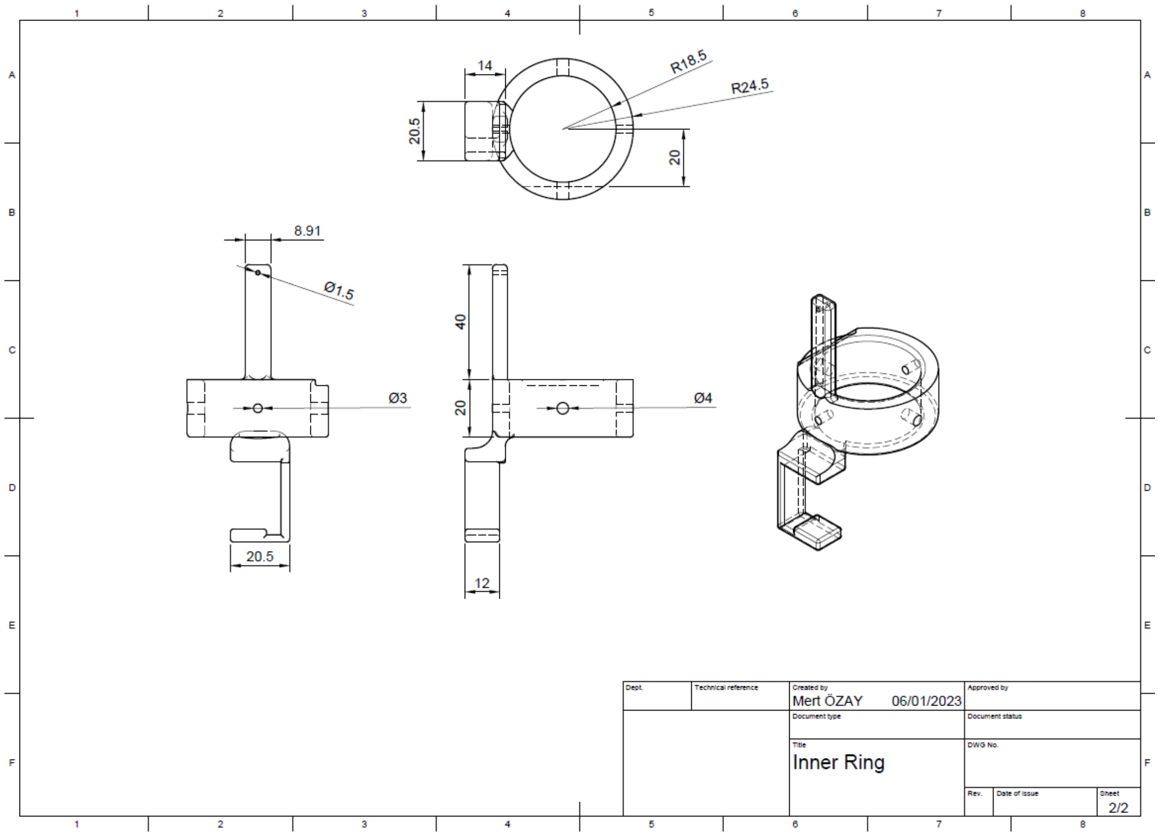
14
R18.5
R24.5
20.5
20
8.91
Ø1.5
Ø3
40
20
Ø4
20.5
12
Dept.
Technical reference
Created by
Mert ÖZAY 06/01/2023
Approved by
Document type
Document status
Title
Inner Ring
DWG No.
Rev.
Date of issue
Sheet
2/2

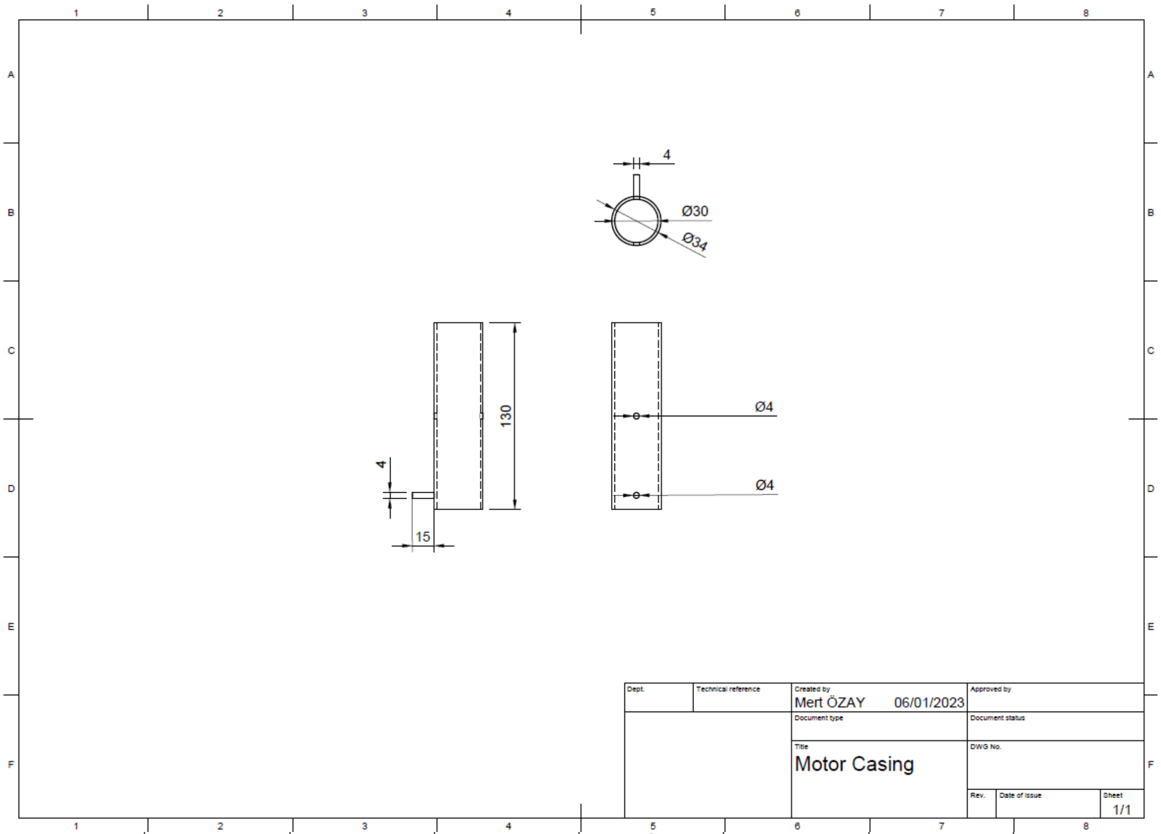
4
Ø30
Ø34
130
Ø4
Ø4
4
15
Created by
Mert ÖZAY 06/01/2023
Title
Motor Casing
Sheet
1/1

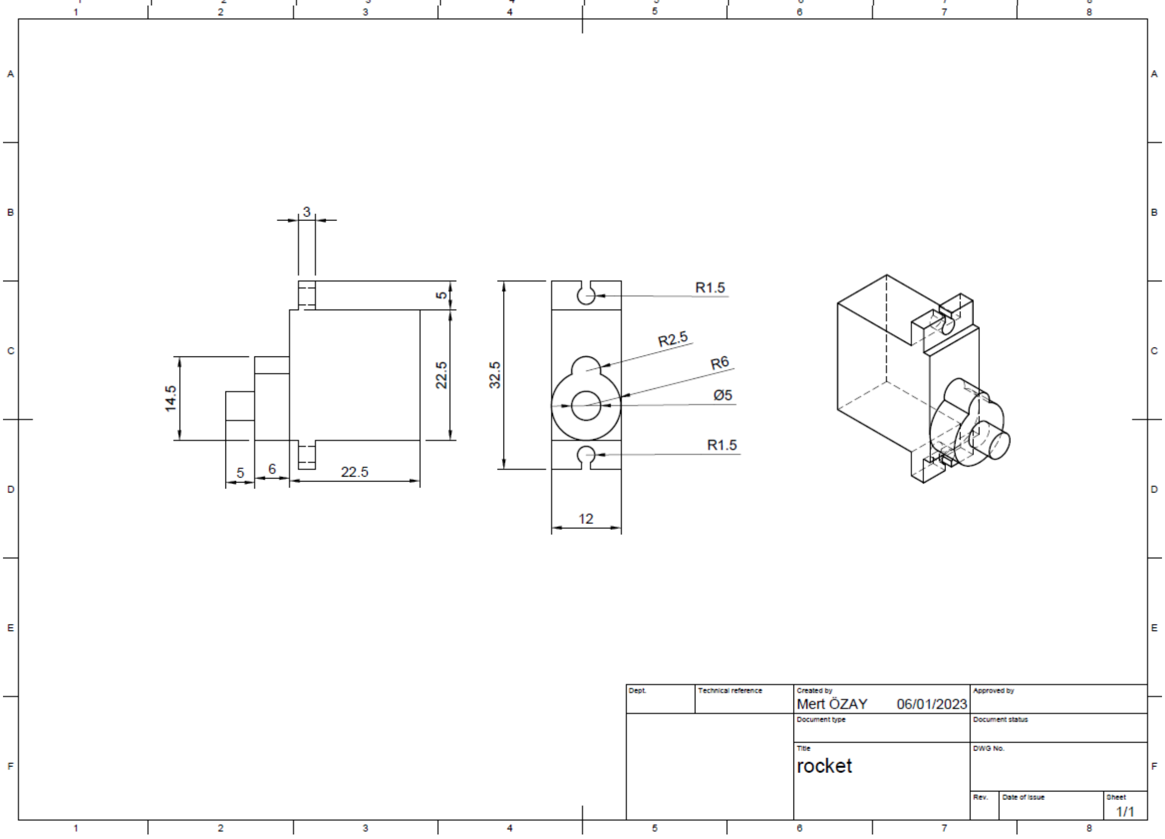
3
5
22.5
14.5
5
6
22.5
32.5
R1.5
R2.5
R6
Ø5
R1.5
12
Created by
Mert ÖZAY 06/01/2023
Title
rocket
Sheet
1/1